Discussion

Many chemicals, including polycyclic aromatic hydrocarbons and estrogens, are metabolically activated to form quinones. ROS such as superoxide, hydrogen peroxide, and, ultimately, reactive hydroxyl radicals are generated through redox cycling between the *o*-quinone and its semiquinone radical and attack cellular macromolecules, including DNA, to generate oxidative DNA damage such as 8-oxodG (*27*). Similarly, 4-OHEN, a major metabolite of EN, autoxidizes to the *o*-quinone without enzymatic or metal ion catalysis (*7*). ROS generated during redox cycling between 4-OHEN-*o*-quinones and their semiquinones cause oxidative DNA damage; indeed, increased formation of 8-oxodG was observed when calf thymus DNA was reacted directly with 4-OHEN (*14*). In mice treated orally with EN, significant increases of 8-oxodG were observed in the liver and uterus using LC/MS/MS (Table 1). A similar result was observed when 4-OHEN was injected directly into the mammary fat pads of rats (*12*). These results indicated that oxidative DNA damage occurs in reproductive organs. ROS generated by equine estrogen and its metabolite may contribute to the process of equine estrogen carcinogenesis.

Women receiving HRT take Premarin at a dose 0.625 (~0.01 mg/kg/day) or 1.25 mg/day (~0.021 mg/kg/day). Because equine estrogens present in Premarin are approximately 40%, women get equine estrogens 0.004 or 0.0084 mg/kg/day. Although the doses (5.0 and 50 mg/kg/day) used in this animal experiment were in excess than the daily dose for women, women receive HRT over 5 years. Therefore, to determine the capability of forming EN-induced oxidative DNA damage in a short period (1 or 2 weeks), high doses were used in this experiment, as reported that other research groups treated a high dose of 4-OHEN (3.1 mg/kg) to rats (*12*). Although the increases of hepatic and uterine 8-oxodG level were observed with both the wild-type and the *Xpc*-KO mice, the 8-oxodG level for 50 mg/kg EN treatment was similar or slightly higher than that observed with 5 mg/kg EN treatment. Such excessive EN doses may give overcapacity for the metabolizing enzymes to produce 4-OHEN, a precursor of forming ROS. The high level of hepatic 8-oxodG observed after 1 week of treatment (5.0 or 50 mg/kg) was subsequently decreased at 2 week. The decrease of hepatic 8-oxodG over time may occur by repair enzymes induced after EN treatment. Our results encourage treating animals for longer periods with low EN doses for predicting the capability of forming oxidative damage in women.

Xpc is a factor involved in the recognition of a variety of bulky DNA-distorting lesions in nucleotide excision repair (*22*) and may also be associated with repair of 8-oxodG (*23*). If *Xpc* is involved in the repair of 8-oxodG, then the lesions should remain in the tissues of *Xpc*-KO mice for considerably longer than in the tissues of wild-type mice. When EN was administered to both *Xpc*-KO and wild-type mice, a significantly higher formation of 8-oxodG was detected only in liver of *Xpc*-KO mice treated with 50 mg/kg; no significant difference in 8-oxodG levels was observed between them with other doses and/or tissues (Table 1). Our results indicate that *Xpc* may not have a primary role in the repair of 8-oxodG.

In *Xpc*-KO and wild-type mice treated only with the vehicle, the levels of 8-oxodG in the uterus were 3.9 and 2.1 times, respectively, higher than that observed in the liver. The uterus is a principal producer of steroid hormones, including estrogen. Estrogen metabolites are known to produce free radicals during redox cycling, generating oxidative DNA damage, including 8-oxodG (*28*). ROS generated by steroid metabolites may be the cause of the increased background level of 8-oxodG in the uterus.

In conclusion, our results indicate that oxidative DNA damage induced by equine estrogen in reproductive organs may contribute to the process of equine estrogen carcinogenesis and increase the risk of developing reproductive cancer in women receiving HRT.

Acknowledgment. This study was supported by Grant ES012408 from the National Institute of Environmental Health Sciences, Grants-in-Aid for scientific research 18101003 from the Ministry of Education, Culture, Sports, Science and Technology of Japan, and Grants-in-Aid for scientific research from the Ministry of Health, Labor and Welfare of Japan.

References

(1) Bolton, J. L., Pisha, E., Zhang, F., and Qiu, S. (1998) Role of quinoids in estrogen carcinogenesis. *Chem. Res. Toxicol. 11*, 1113–1127.
(2) Colditz, G. A., Hankinson, S. E., Hunter, D. J., Willett, W. C., Manson, J. E., Stampfer, M. J., Hennekens, C. H., Rosner, B., and Speizer, F. E. (1995) The use of estrogens and progestins and the risk of breast cancer in postmenopausal women. *N. Engl. J. Med. 332*, 1589–1593.
(3) Grodstein, F., Stampfer, M. J., Colditz, G. A., Willett, W. C., Manson, J. E., Joffe, M., Rosner, B., Fuchs, C., Hankinson, S. E., Hunter, D. J., Hennekens, C. H., and Speizer, F. E. (1997) Postmenopausal hormone therapy and mortality. *N. Engl. J. Med. 336*, 1769–1775.
(4) Lacey, J. V., Jr., Mink, P. J., Lubin, J. H., Sherman, M. E., Troisi, R., Hartge, P., Schatzkin, A., and Schairer, C. (2002) Menopausal hormone replacement therapy and risk of ovarian cancer. *J. Am. Med. Assoc. 288*, 334–341.
(5) Shen, L., Qiu, S., Chen, Y., Zhang, F., van Breemen, R. B., Nikolic, D., and Bolton, J. L. (1998) Alkylation of 2′-deoxynucleosides and DNA by the Premarin metabolite 4-hydroxyequilenin semiquinone radical. *Chem. Res. Toxicol. 11*, 94–101.
(6) Ding, S., Shapiro, R., Geacintov, N. E., and Broyde, S. (2003) Conformations of stereoisomeric base adducts to 4-hydroxyequilenin. *Chem. Res. Toxicol. 16*, 695–707.
(7) Zhang, F., Chen, Y., Pisha, E., Shen, L., Xiong, Y., van Breemen, R. B., and Bolton, J. L. (1999) The major metabolite of equilin, 4-hydroxyequilin, autoxidizes to an *o*-quinone which isomerizes to the potent cytotoxin 4-hydroxyequilenin-*o*-quinone. *Chem. Res. Toxicol. 12*, 204–213.
(8) Yasui, M., Matsui, S., Laxmi, Y. R. S., Suzuki, N., Kim, S. Y., Shibutani, S., and Matsuda, T. (2003) Mutagenic events induced by 4-hydroxyequilin in *supF* shuttle vector plasmid propagated in human cells. *Carcinogenesis 24*, 911–917.
(9) Suzuki, N., Yasui, M., Laxmi, Y. R. S., Ohmori, H., Hanaoka, F., and Shibutani, S. (2004) Translesion synthesis past equine estrogen-derived 2′-deoxycytidine DNA adducts by human DNA polymerases *η* and *κ*. *Biochemistry 43*, 11312–11320.
(10) Yasui, M., Laxmi, Y. R. S., Ananthoju, S. R., Suzuki, N., Kim, S. Y., and Shibutani, S. (2006) Translesion synthesis past equine estrogen-derived 2′-deoxyadenosine DNA adducts by human DNA polymerases *η* and *κ*. *Biochemistry 45*, 6187–6194.
(11) Yasui, M., Suzuki, N., Liu, X., Okamoto, Y., Kim, S. Y., Laxmi, Y. R. S., and Shibutani, S. (2007) Mechanism of translesion synthesis past an equine estrogen-DNA adduct by Y-family DNA polymerases. *J. Mol. Biol. 371*, 1151–1162.
(12) Zhang, F., Swanson, S. M., van Breemen, R. B., Liu, X., Yang, Y., Gu, C., and Bolton, J. L. (2001) Equine estrogen metabolite 4-hydroxyequilenin induces DNA damage in the rat mammary tissues: Formation of single-strand breaks, apurinic sites, stable adducts, and oxidized bases. *Chem. Res. Toxicol. 14*, 1654–1659.
(13) Embrechts, J., Lemiere, F., Van Dongen, W., Esmans, E. L., Buytaert, P., Van Marck, E., Kockx, M., and Makar, A. (2003) Detection of estrogen DNA-adducts in human breast tumor tissue and healthy tissue by combined nano LC-nano ES tandem mass spectrometry. *J. Am. Soc. Mass Spectrom. 14*, 482–491.
(14) Chen, Y., Shen, L., Zhang, F., Lau, S. S., van Breemen, R. B., Nikolic, D., and Bolton, J. L. (1998) The equine estrogen metabolite 4-hydroxyequilenin causes DNA single-strand breaks and oxidation of DNA bases in vitro. *Chem. Res. Toxicol. 11*, 1105–1111.
(15) Han, X., and Liehr, J. G. (1995) Microsome-mediated 8-hydroxylation of guanine bases of DNA by steroid estrogens: Correlation of DNA damage by free radicals with metabolic activation to quinones. *Carcinogenesis 16*, 2571–2574.

(16) Chen, Y., Liu, X., Pisha, E., Constantinou, A. I., Hua, Y., Shen, L., van Breemen, R. B., Elguindi, E. C., Blond, S. Y., Zhang, F., and Bolton, J. L. (2000) A metabolite of equine estrogens, 4-hydroxyequilenin, induces DNA damage and apoptosis in breast cancer cell lines. *Chem. Res. Toxicol. 13*, 342–350.

(17) Zhang, F., Yao, D., Hua, Y., van Breemen, R. B., and Bolton, J. L. (2001) Synthesis and reactivity of the catechol metabolites from the equine estrogen, 8,9-dehydroestrone. *Chem. Res. Toxicol. 14*, 754–763.

(18) Liu, X., Yao, J., Pisha, E., Yang, Y., Hua, Y., van Breemen, R. B., and Bolton, J. L. (2002) Oxidative DNA damage induced by equine estrogen metabolites: Role of estrogen receptor α. *Chem. Res. Toxicol. 15*, 512–519.

(19) Shibutani, S., Takeshita, M., and Grollman, A. P. (1991) Insertion of specific bases during DNA synthesis past the oxidation-damaged base 8-oxodG. *Nature 349*, 431–434.

(20) Moriya, M. (1993) Single strand shuttle phagemid for mutagenesis studies in mammalian cells: 8-oxoguanine in DNA induces targeted G:C → T:A transversion in simian kidney cells. *Proc. Natl. Acad. Sci. U.S.A. 90*, 1122–1126.

(21) Tan, X., Grollman, A. P., and Shibutani, S. (1999) Comparison of the mutagenic properties of 8-oxo-7,8-dihydro-2′-deoxyadenosine and 8-oxo-7,8-dihydro-2′-deoxyguanosine DNA lesions in mammalian cells. *Carcinogenesis 20*, 2287–2292.

(22) Sands, A. T., Abuin, A., Sanchez, A., Conti, C. J., and Bradley, A. (1995) High susceptibility to ultraviolet-induced carcinogenesis in mice lacking XPC. *Nature 14*, 162–165.

(23) D'Errico, M., Parlanti, E., Teson, M., Bernardes de Jesus, B. M., Degan, P., Calcagnile, A., Jaruga, P., Bjørås, M., Crescenzi, M., Pedrini, A. M., Egly, J., Zambruno, G., Stefanini, M., Dizdaroglu, M., and Dogliotti, E. (2006) New functions of XPC in the protection of human skin cells from oxidative damage. *EMBO J. 25*, 4305–4315.

(24) Wang, L., Hirayasu, K., Ishizawa, M., and Kobayashi, Y. (1994) Purification of genomic DNA from human whole blood by isopropanol-fractionation with concentrated NaI and SDS. *Nucleic Acids Res. 22*, 1774–1775.

(25) Collins, A., and Gedik, C. M. (2005) Establishing the background level of base oxidation in human lymphocyte DNA: results of an interlaboratory validation study ESCODD (European Standards Committee on Oxidative DNA Damage). *FASEB J. 19*, 82–84.

(26) Schuler, D., Ottenedер, M., Sagelsdorff, P., Eder, E., Gupta, R. C., and Lutz, W. K. (1997) Comparative analysis of 8-oxo-2′-deoxyguanosine in DNA by ^{32}P-postlabeling and electrochemical detection. *Carcinogenesis 18*, 2367–2371.

(27) Bolton, J. L., Trush, M. A., Penning, T. M., Dryhurst, G., and Monks, T. J. (2000) Role of quinones in toxicology. *Chem. Res. Toxicol. 13*, 135–160.

(28) Han, X., and Liehr, J. G. (1994) 8-Hydroxylation of guanine bases in kidney and liver DNA of hamsters treated with estradiol: Role of free radicals in estrogen-induced carcinogenesis. *Cancer Res. 54*, 5515–5517.

TX700428M

Arch Environ Contam Toxicol (2008) 55:199–209
DOI 10.1007/s00244-007-9110-5

Aryl Hydrocarbon Receptor and Estrogen Receptor Ligand Activity of Organic Extracts from Road Dust and Diesel Exhaust Particulates

Kentaro Misaki · Masato Suzuki · Masafumi Nakamura · Hiroshi Handa · Mitsuru Iida · Teruhisa Kato · Saburo Matsui · Tomonari Matsuda

Received: 8 August 2007 / Accepted: 3 December 2007 / Published online: 8 January 2008

Abstract A wide variety of contaminants derived from diesel and gasoline engines, tire, asphalt, and natural organic compounds is found in road dust. Polycyclic aromatic compounds (PACs) are the important toxic targets among various contents in road dust and diesel exhaust particulates (DEPs), and endocrine-disrupting activity of PACs was suggested. In the present study, aryl hydrocarbon receptor (AhR) ligand activity was confirmed in the extract of both road dust and DEPs. In the separation of the extracts for both road dust and DEPs with reversed-phase HPLC, it was found that polar fractions contributed to significant AhR ligand activity in both a mouse hepatoma (H1L1) cell system and a yeast system. Furthermore, the contribution of these polar fractions was higher in DEPs than in road dust, probably because of the greater concentration of oxy-PAHs in DEPs than in road dust. The contribution of contaminants associated with the polar region to AhR ligand activity was also evident following the separation of road dust with normal-phase HPLC. Additionally, remarkable estrogen receptor (ER) ligand activity was detected in the highly polar region separated with normal-phase HPLC. It is suggested that many unknown AhR or ER ligand active compounds are contained in the polar region.

K. Misaki · M. Suzuki
Department of Environmental Engineering, Graduate School of Engineering, Kyoto University, Yoshida-honmachi, Sakyo-ku, Kyoto 606-8501, Japan

K. Misaki · S. Matsui · T. Matsuda (✉)
Department of Technology and Ecology, Graduate School of Global Environmental Studies, Kyoto University, Yoshida-honmachi, Sakyo-ku, Kyoto 606-8501, Japan
e-mail: matsuda@z05.mbox.media.kyoto-u.ac.jp

M. Nakamura · H. Handa
Hiyoshi Corporation, 908 Kitanosho-cho, Omihachiman, Shiga 523-8555, Japan

M. Iida · T. Kato
Otsuka Pharmaceutical Company, Ltd, 224-18 Ebisuno Hiraishi, Kawauchi-cho, Tokushima 771-0195, Japan

Road dust is an important nonpoint pollution source because it is transported through storm water runoff, which is generally discharged into aquatic environments without treatment (Lee et al. 2005a, b). Road dust includes various metals and inorganic and organic compounds derived from diesel and gasoline engines (Rogge et al. 1993b; Crepineau et al. 2003).

To the surface of the carbon core in diesel exhaust particulates (DEPs), various contaminants are adhered. These contaminants include organic substances, metals (Fe, Cu, Co, V, etc.), and sulfates, nitrates, and ammonium salts of these acids (Mcdonald et al. 2004). The main organic compounds included in an extraction solution of DEPs with organic solvent are aliphatic compounds (aliphatic hydrocarbons and aliphatic acids), polycyclic aromatic compounds (PACs), steranes and hopanes derived from natural compounds, phthalic acid esters, etc. PACs include polycyclic aromatic hydrocarbons (PAHs), oxygenated PAHs (oxy-PAHs; polycyclic aromatic ketones [PAKs], polycyclic aromatic quinones [PAQs], hydroxylated PAHs [hydroxy-PAHs], polycyclic aromatic carboxaldehydes, polycyclic aromatic carboxylic acids, polycyclic aromatic lactones, polycyclic aromatic anhydrides), and nitrogenated aromatic compounds such as nitro-PACs and heterocyclic amines (Rogge et al. 1993a; Alsberg et al. 1985; Casellas et al. 1995; Hannigan et al. 1998; Pedersen et al. 2005; Fernandez et al. 1992; Kannan et al. 2000). Besides contents derived from diesel and

gasoline engines, road dust is also thought to include natural resins, polyethylene glycol ethers, and high-ring-number PACs derived from tires and asphalt, and natural organic compounds transferred from airborne particulates, etc., are also thought to be included (Rogge et al. 1993b).

PACs are important toxic targets among various contents in road dust and DEPs and accumulate in the sediment of aquatic environments via storm water runoff (Kannan et al. 2000; Fernandez et al. 1992), and some wildlife and humans have the risk of exposure to them. Many studies of PAC mutagenicity and carcinogenicity have been reported (Durant et al. 1996; Machala et al. 2001a; IARC 1983), however, studies on endocrine-disrupting activity of PACs are few.

Since the 1990s, the importance of endocrine-disrupting activity of environmental contaminants has been emphasized (Colborn et al. 2004; Vos et al. 2000). Endocrine-disrupting phenomena by diesel exhaust have often been reported for male mice and rats (Yoshida et al. 2000; Tsukue et al. 2001, 2004; Watanabe et al. 1999; Wells et al. 1997; Matsumoto et al. 1986), and diesel exhaust has been connected primarily with antiandrogenic and estrogenic activity (Okamura et al. 2004; Kizu et al. 2003; Ohtake et al. 2003; Machala et al. 2001b). It was also reported that the mass of storage tissue and production of gametes decreased in marine mollusks exposed to diesel oil (Moore et al. 1989). These endocrine disruption activities of diesel exhaust and oil are likely to be caused by PACs such as benzo[*a*]pyrene (B[a]P), however it has not yet been determined what compounds contribute most to this activity (Okamura et al. 2004; Kizu et al. 2003; Ohtake et al. 2003, 2007; Machala et al. 2001b). Some PACs and hydroxy-PAHs showed estrogenic ligand activity for culture cells via direct binding to the estrogen receptor (ER) (Machala et al. 2001b; Clemons et al. 1998; Kamiya et al. 2005; Hirose et al. 2001; van Lipzig et al. 2007). It is also supposed that PACs cause endocrine disruption via the aryl hydrocarbon receptor (AhR) and that the induction of enzymes such as CYP1A1 mediated by AhR is likely to be one of the biomarkers for endocrine disruption (Okamura et al. 2004; Kizu et al. 2003; Ohtake et al. 2003, 2007; Machala et al. 2001b). The association between AhR ligand activity and the inhibition of androgen receptor (AR) response gene expression has been reported (Okamura et al. 2004; Kizu et al. 2003). The pathway via ER-AhR binding interaction has also been predicted for endocrine-disrupting activity in male reproductive organs under PAC exposure (Ohtake et al. 2003). Moreover, the phenomenom that degradation of hormone receptors (e. g., ER and AR) can be mediated by the AhR ligand-dependent ubiquitin-proteosome system (Ohtake et al. 2007) has also been reported.

A ligand activates AhR and AhR transfers into the nucleus and forms the AhR complex by binding with the AhR nuclear translocator. The AhR complex binds xenobiotic response elements and mediates the expression regulation of gene expression, including specific CYPs, glutathione-*S*-transferases, NAD(P)H-dependent quinone oxidoreductase 1, growth factors, and cytokines (Schmidt et al. 1996; Giesy et al. 2002). Many environmental pollutants or natural substances (dioxins, PAHs, tryptophan derivatives, etc.) bind and activate the AhR as exogeneous or endogeneous ligands (Miller et al. 1999; Ziccardi et al. 2002; Clemons et al. 1998; Machala et al. 2001a, b; Till et al. 1999; Jones et al. 1999; Okamura et al. 2004; Bols et al. 1999; Chou et al. 2006, 2007; Denison et al. 2002; Adachi et al. 2001). In our previous study, the AhR ligand activity of oxy-PAHs, such as PAKs and PAQs more polar than PAHs, and the contribution of these polar compounds to the AhR ligand activity of atmospheric samples were reported (Misaki et al. 2007a, b; Machala et al. 2001b).

It is significant to grasp the generous distribution of PAC contents and the hormone receptor ligand activity depending on chemical properties such as polarity in fractions separated using HPLC, from road dust and DEP extracts, for the purpose of toxicological quality control corresponding to compound groups in storm water runoff as a nonpoint source of aquatic environments (Lee et al. 2005a–c; Kawanishi et al. 2004). However, the overvall distribution is unknown in detail (Clemons et al. 1998). In the present study, separation of extracts of both road dust and DEPs was performed with reversed-phase HPLC, and AhR ligand activity for these fractions was measured. AhR ligand activity was evaluated with both luciferase activity in mouse hepatoma (H1L1) cells (chemical activated luciferase gene expression [CALUX] assay) (Ziccardi et al. 2002; Denison et al. 1998) and β-galactosidase activity from a reporter plasmid in yeast, engineered to express human AhR and AhR nuclear translocator proteins (Miller et al. 1999). Additionally, AhR and ER ligand activity was investigated for fractions of road dust separated with the combination of three kinds of columns (Sephadex and normal- and reversed-phase columns). ER ligand activity was evaluated using Chinese hamster ovary (CHO-K1) cells transfected with the human ER gene (Iida et al. 2003; Kojima et al. 2003; Kitamura et al. 2005).

Materials and Methods

Chemicals

DMSO, methanol, acetonitrile, hexane, and chloroform, HPLC grade, were purchased from Wako Chemical (Osaka, Japan). Most PACs were supplied by Sigma-Aldrich Co. (St. Louis, MO, USA). The other PACs were supplied by Nacalai Tesque Co. (Tokyo), Wako Chemical, Tokyo Kasei Co. (Tokyo), and Promochem (Wesel,

Germany). The purity of many PACs was 99%–100%. The purities of benzo[*b*]fluoranthene, benzo[*k*]fluoranthene, anthraquinone, 7,12-benz[*a*]anthracenequinone, and β-naphthoflavone (β-NF) were 98%. The purities of triphenylene, dibenz[*a*,*h*]anthracene, phenalenone, and 5,12-naphthacenequinone were 97%.

11*H*-Benzo[*a*]fluoren-11-one, 11*H*-benzo[*b*]fluoren-11-one, and 6*H*-benzo[*c*,*d*]pyren-6-one were synthesized as described previously (Misaki et al. 2007). These compounds were purified by column chromatography and recrystallization. The purities of these three synthesized compounds were >99% as judged by HPLC.

Sampling and Extraction

Road dust was collected from Meishin Expressway (Yokaichi IC–Ryuoh IC–Ritto IC) in an urban area of the southern part of Lake Biwa, Japan, at September 28, 2001. The traffic density between 7 AM and 7 PM on October 7, 1999, was 38,598 vehicles/12 h at the sampling site between Yokaichi IC and Ryuoh IC and 46,974 vehicles/12 h at the sampling site between Ryuoh IC and Ritto IC. Road dust was collected and transported to the laboratory as described previously (Lee et al. 2005b). After air-drying in the dark, 5 kg of the sample was sieved through a 500-μm stainless-steel sieve (JISZ 8801, Iida, Japan) to remove gravel, leaf material, glass, and other debris, then ~700 g of sieved sample was separated. Extraction of organic contents from the sieved sample was done using an accelerated solvent extractor (ASE-200; Dionex). The sieved sample (5 g) with 40 g of glass beads was placed in each extraction cell of the ASE. Extraction was carried out twice with dichloromethane under conditions of 100 atm, 100°C for 5 min, static time of 5 min, purge time of 90 s, and flush of 60%. The extraction solution was evaporated using a rotary vaccum evaporator, and 13.5 g of extract was obtained.

DEPs were obtained from an Isuzu Model A4JB1 engine (2740 cm^3, 4-cylinder direct injection type) running on a chassis dynamometer under loads of 30% (torque, 10 kg-m; 1500 rpm) of a maximum engine load fixed at 2000 rpm (Okamura et al. 2004). Exhaust gas containing particulate matter was diluted with clean air in a dilution tunnel, and the DEPs accumulated in the tunnel were collected. Twenty milligrams of DEPs was ultrasonically extracted with 160 ml of chloroform for 10 min and the solution was evaporated to dryness in vacuo.

Separation of Sample Extracts

An extract sample of road dust, 5 mg, was dissolved in 200 μl of DMSO (3% $CHCl_3$) and filtered with a 0.2-μm polytetrafluoroethylene (PTFE) filter (liquid chromatography 13CR; Pall Co., East Hills, NY, USA). Fifty microliters of filtered solution was injected into an analytical HPLC column (Shimpack FC-ODS; ø4.6 × 150 mm; Shimadzu, Kyoto, Japan). An extract sample of DEPs, 5 mg, was dissolved in 200 μl of DMSO (3% $CHCl_3$) and filtered with a 0.2-μm PTFE filter. Fifty microliters of 10 × diluted solution of the filtrated solution with DMSO was used for injection.

Separation Conditions Using HPLC

The separation of injected solution, 50 μl (equivalent to ~1 mg of road dust extract and ~100 μg of DEP extract), using a reversed-phase analytical HPLC column, was eluted with water-acetonitrile as the mobile phase (a linear gradient of water containing 20%–100% acetonitrile for 0–20 min and 100% acetonitrile for 20–80 min) over 80 min at a flow rate of 1.0 ml/min. A fraction was collected every 1 min, evaporated, and dissolved in 20 μl of DMSO. The fraction solution from the road dust extract was subjected intact to yeast and CALUX assay, and the fraction solution from the DEP extract was subjected intact to yeast and as a 10 × diluted solution to CALUX assay. The reversed-phase HPLC system constituted an LC-10ATvp pump, a SIL-10ADvp UV-VIS detector at 254 nm, an SCL-10Avp system controller (Shimadzu), and a fraction collector (SF-2120; Advantec, Tokyo). AhR ligand activity is expressed as β-NF equivalent concentration. The β-NF equivalent concentration (as a quantitative index) to express observed AhR ligand activity was defined as the β-NF concentration at which the activity value was the same as the value for each fraction.

Extract of road dust, 20 mg, was dissolved in 1 ml of mixture solvent of hexane-chloroform-methanol (1:1:1). The solution was injected to a Sephadex HPLC column (Sephadex LH-20; ø10 × 250 mm; GL Sciences Inc., Tokyo) and eluted with hexane-chloroform-methanol (1:1:1) as the mobile phase (isocratic) over 40 min at a flow rate of 2.5 ml/min. Four hundred microliters of the fraction solution (2.5 ml) collected every 1 min was evaporated and dissolved in 20 μl of DMSO. This solution was subjected intact to AhR assay with yeast and ER assay. This separation was repeated and the fractions showing AhR ligand activity (fractions 5–20) were pooled and evaporated. Twenty milligrams of the residue was dissolved in 1 ml of mixture solvent of hexane-chloroform (85:15). Six hundred microliters of the solution (equivalent to 12 mg of the residue) was injected into a normal-phase HPLC column (Wakogel LC30H; ø10 × 250 mm; Wako) and was eluted with hexane-chloroform as the mobile phase (a linear gradient of hexane containing 15%–100% chloroform for

0–30 min and 100% chloroform for 30–100 min) over 100 min at a flow rate of 2.5 ml/min. One hundred microliters of the fraction solution (2.5 ml) collected every 1 min was evaporated and dissolved in 20 µl of DMSO. This solution was subjected intact to AhR assay with yeast and as a 10 × diluted solution to ER assay. The Sephadex and normal-phase HPLC system constituted an LC-10ADvp pump, a SIL-10ADvp UV-VIS detector at 254 nm, an CT-10Avp column oven at 40C, and an SCL-10Avp system controller (Shimadzu). Two and four-tenths milliliters of the fraction 9 solution was evaporated and the residue was dissolved in 70 µl of DMSO. Fifty microliters of the solution was injected into a reversed-phase HPLC column, and fractionation and AhR assay with yeast were carried out as described above. The UV absorption pattern of these separated fractions showed a similar pattern in at least two handlings.

Yeast Assay

The assay was performed as described previously (Misaki et al. 2007b). *Saccharomyces cerevisiae* strain YCM3 was grown in synthetic glucose medium at 30°C overnight in a shaking incubator (Miller et al. 1999). The next day 10 µl from the saturated culture was inoculated into glass tubes containing 400 µl of a synthetic 2% galactose medium. Each fraction solution dissolved in 2 µl of DMSO was added to the medium to achieve a final solvent concentration of 0.5%, followed by 18 h of incubation at 30°C. The yeast exposed to each fraction solution was incubated in a 96-well plate at half-volume scale in glass tubes, for the experiments combining three kinds of columns. Cell densities were determined by reading the absorbance at 595 nm, and 10 µl of the cell suspension was added to 140 µl of Z-buffer (60 mM Na_2HPO_4, 40 mM NaH_2PO_4, 1 mM $MgCl_2$, 10 mM KCl, 2 mM dithiothreitol, and 0.2% Sarkosyl). The reaction was started by adding 50 µl of *o*-nitrophenyl-*β*-D-galactopyranoside (ONPG; 4 mg/ml solution in Z-buffer). Samples were incubated at 37°C for 60 min. Absorbances of the reaction mixture were read in a spectrophotometer at 405 nm. The activity of *β*-galactosidase (referred to as lacZ units) was calculated by the following formula: $412 \times A_{405\ nm}/(400 \times A_{595\ nm} \times$ ml of cell suspension added × minutes of reaction time). The activity is also expressed as *β*-NF equivalent concentration (Adachi et al. 2001; Chou et al. 2006, 2007). The *β*-NF equivalent concentration was defined as the *β*-NF concentration at which the activity value was the same as the value for each fraction. The *β*-NF equivalent concentration was calculated from the dose-response curve of *β*-NF (as a positive standard). The results of yeast assay of these separated fractions showed a similar pattern in at least two experiments.

CALUX Assay

The assay was also performed as described previously (Misaki et al. 2007b). Mouse hepatoma (H1L1.1c2) cells ($\sim 1.5 \times 10^5$ cells/well) were cultured in 96-well culture plates, and each fraction solution dissolved in DMSO was added to the medium to achieve a final solvent concentration of 1% (Ziccardi et al. 2002; Denison et al. 1998). After the plates were incubated at 37°C in 5% CO_2 for 24 h, the cell viability was confirmed under a microscope. Subsequently, the medium was removed and the cells were lysed with 30 µl of lysis buffer. Fifty microliters of luciferin (firefly) solution was added to all assay wells according to protocol (Luciferase Assay System, Promega Co., Madison, WI, USA), then immediately luciferase activity was determined under a Lucy1 luminometer (Anthos Co., Eugendorf, Austria) and is reported as relative light units (RLUs). CALUX assay was done one time.

ER Ligand Activity Assay

ER ligand activity assay was performed as described in previous studies with some modifications (Iida et al. 2003; Kojima et al. 2003; Kitamura et al. 2005). Chinese hamster ovary (CHO-K1) cells (8400 cells/well) were plated in 96-well plates at 84 µl/well at a density of 1×10^5 cells/ml in phenol red-free DMEM/F12 medium supplemented with 5% charcoal dextran-treated FBS. CHO cells were cultured for 24 h at 37C, under 5% CO_2 (Iida et al. 2003; Kojima et al. 2003; Kitamura et al. 2005). Each fraction of DMSO solution was diluted 12.5 times with DMEM/F12 with no supplement, so that the final DMSO concentration was 0.08% (v/v). We transfected cells with 6.25 ng pcDNAER*α* or pcDNAER*β*, 62.5 ng pGL3-tkERE, and 10 ng pcDNA-enhanced green fluorescent protein (EGFP) at 6 µl/well using the transfection reagent FuGene6 (Roche Diagnostics Co., Indianapolis, IN, USA). After a 3-h transfection period, cells were dosed with 10 µl of each diluted fraction solution and cultured for 24 h. The solvent control and 1 nM estradiol (final concentration), which served as the positive control, were incubated in each plate. Following 24 h of culture, green fluorescence radiating from living cells was measured prior to luminescence measurement with a Wallac 1420 ARVO SX multilabel counter (Perkin-Elmer, Boston, MA, USA). Then the luciferase substrate with cell lysis reagent Steady-Glo (Promega Co.) was added to all assay wells in the same plate. The plate was shaken at room temperature for 5 min, then the luciferase activity was determined under a luminometer and is reported as relative light units (RLUs). The results of ER ligand activity assay for these separated fractions showed a similar pattern in at least two experiments.

Results and Discussion

AhR ligand activity was examined with both a mouse hepatoma (H1L1) cell system and a yeast system for fractions separated from DMSO solution of extracts of road dust and DEPs, using reversed-phase (ODS) HPLC (Fig. 1). In the road dust extract (equivalent to ~1 mg), the polar region (fractions ≤ 30) as well as the hydrophobic region (approximately fractions 31–45) contributed to total AhR ligand activity in the H1L1 cell system. Significant activities were observed in several much later fractions (fractions > 45). Several AhR ligand active compounds including high-ring PAHs or natural compounds, with later retention times and derived from tires or asphalt, also may contribute to the AhR ligand activity of road dust (Rogge et al. 1993b). The contribution of the region including

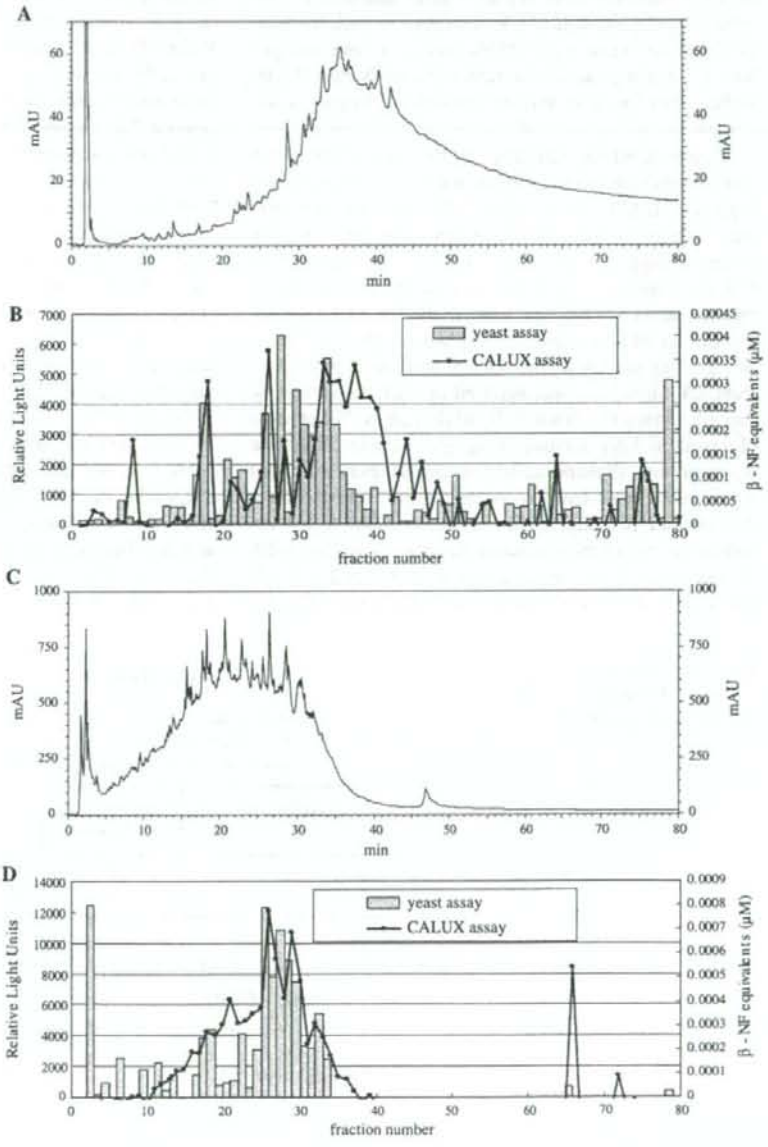

Fig. 1 AhR activities in yeast assay and CALUX assay for exposure to each fraction separated on an ODS column from extracts of road dust and diesel exhaust particulates (β-NF equivalents for yeast assay and relative light units for CALUX assay). A UV absorption for road dust. B AhR ligand activity for road dust. C UV absorption for diesel exhaust particulates. D AhR ligand activity for diesel exhaust particulates

PAHs to the total AhR ligand activity was higher in the H1L1 system than in the yeast system. This is probably because the speed of uptake and metabolism of hydrophobic contents (such as PAHs) are slower for yeast than for mouse hepatoma cells (Miller et al. 1999; Misaki et al. 2007b). However, in DEP extract (equivalent to ~100 μg), fractions with later retention times (fractions ≥ 40) did not show significant AhR ligand activity except for fractions 66 and 72. It was observed that polar compounds were included relatively more in DEP extract than in road dust extract, by the strength of UV absorption in each fraction. This may be because oxy-PAHs generated from automobiles are decomposed on the road more easily than PAHs, while DEPs include various oxy-PAHs (Rogge et al. 1993a).

Moreover, minute separation of the constituents of the dichloromethane extract of road dust was carried out using Sephadex (LH20), normal-phase (silica gel), and reversed-phase (ODS) column HPLC, in that order (Fig. 2). AhR ligand activity in yeast assay and ER ligand activity in Chinese hamster ovary (CHO-1) cell assay were examined for the fractions in the separation. In the first separation for the extract of road dust, 20 mg with Sephadex HPLC, neither AhR nor ER ligand activity was found, but significant UV absorption was detected in fractions with early retention times (fractions 1–4), while both activities were observed in later fractions (Fig. 3). Nonactive aliphatic hydrocarbons, aliphatic acids, low-ring-number PACs, and so on are probably removed as early-eluted components by this method (Casellas et al. 1995). In addition, for the residue in evaporation of active fractions (fractions 5–20; 12 mg), separation with normal-phase HPLC and AhR and ER assay of these fractions were performed (Fig. 4). Retention times of representative PACs in this normal-phase HPLC were also examined (Table 1), although the concentration of each PAC was not examined in this study. The existence of these PACs in road dust is fully expected from analytical data previously reported for atmospheric environments (Rogge et al. 1993a; Alsberg et al. 1985; Casellas et al. 1995; Hannigan et al. 1998; Pedersen et al. 2005; Fernandez et al. 1992). In the second separation of road dust extract using normal-phase HPLC, the AhR ligand active peak was observed in fraction 8–11, where many PAH standards are included in the same fractions. Weak ER ligand activity was shown in fraction 8–11, and this is thought to be generated from PAHs such as B[a]P, benz[*a*]anthracene, and chrysene, showing weak ER ligand activity (Machala et al. 2001b; Clemons et al. 1998). AhR ligand activity observed in fractions 12–19 was probably derived from PAKs and PAQs (they were thought to be contained in these fractions; Table 1). AhR ligand activity was also observed in fractions 20–50, and remarkable ER ligand activity was observed in the region of fractions 37–43 and 48–54. It has not been determined what compounds contribute to the AhR and ER ligand activity in fractions 37–43. Hydroxy-PAHs are candidates contributing to these activities in these fractions because several hydroxy-PAHs have both AhR and ER ligand activity (Kamiya et al. 2005; Hirose et al. 2001; van Lipzig et al. 2007; Burczynski et al. 2000). It has not been elucidated what compounds contribute to the ER ligand activity of fraction 48–54. Polycyclic aromatic carboxylic acids, estradiol derived from natural compounds, and possibly hydroxylated cyclic aliphatic hydrocarbons like estradiol are candidates for ER ligand activity in these fractions (Hannigan et al. 1998; Casellas et al. 1995; Fernandez et al. 1992; Kamiya et al.

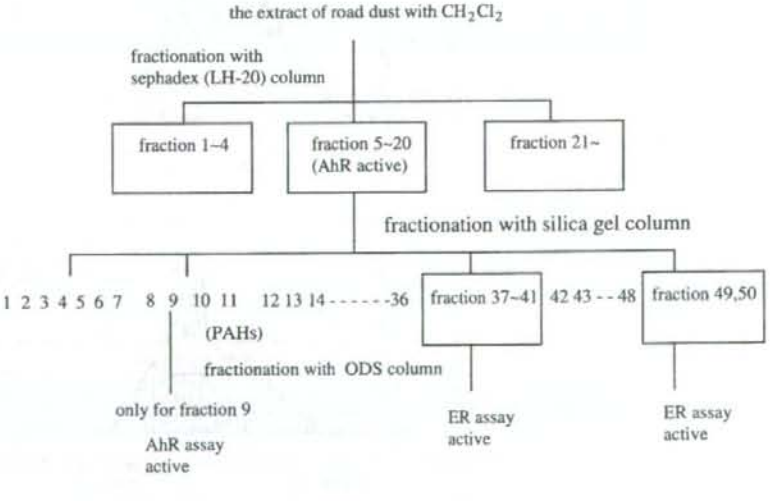

Fig. 2 Flow of the separation of extracts of road dust and AhR and ER assays for fractions

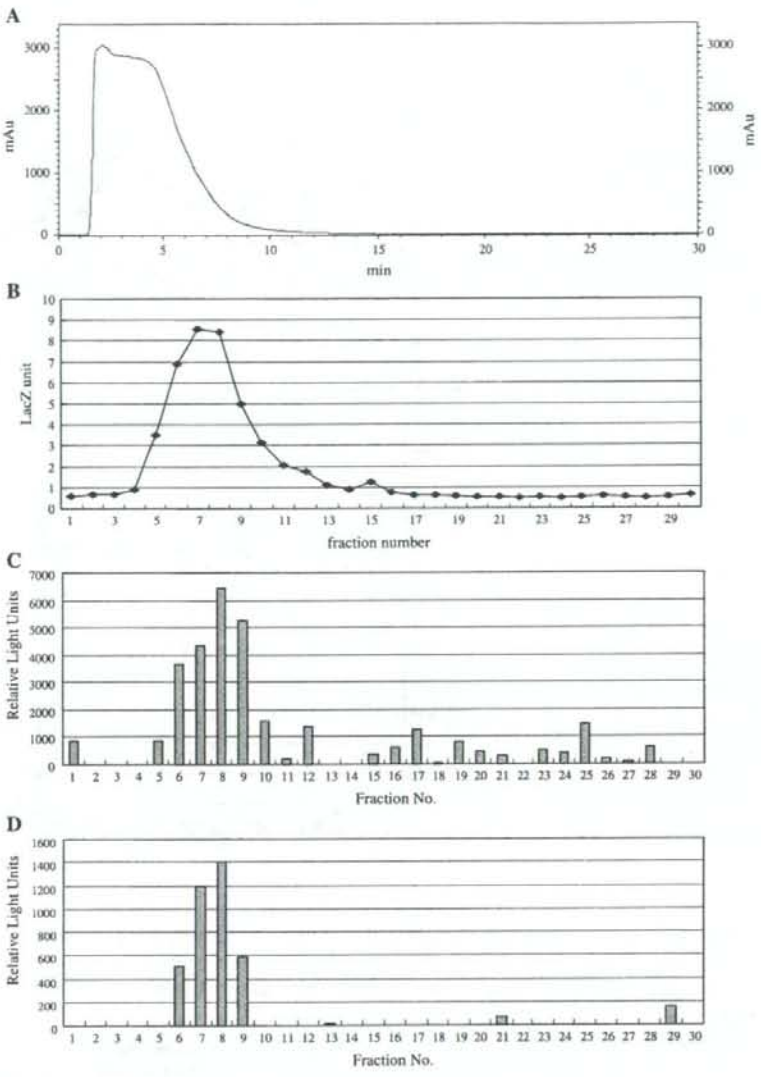

Fig. 3 First separation of extracts of road dust with a Sephadex column and bioassay of fractions. A UV absorption at 254 nm. B AhR assay. C ER α assay. D ER β assay

2005; van Lipzig et al. 2005). Further separation of fraction 9 with reversed-phase HPLC was performed and a clear UV chromatogram was observed at the retention times including PAHs (Fig. 5).

It was reported that the formation of many kinds of oxy-PAHs were observed in the oxidation process of PAHs (Nikolaou et al. 1984; Letzel et al. 2001; Choi et al. 2003), and the toxicological significance of polar compounds in environments is predicted (Matsumoto et al. 1986; Kannan et al. 2000; Clemons et al. 1998; Choi et al. 2003). In our previous study AhR ligand activities of oxy-PAHs such as PAKs and PAQs are lower than representative AhR ligand active PAHs (benzo[*k*]fluoranthene, dibenz[*a*,*h*]anthracene, B[a]P etc.), and the calculated contribution of representative PAKs and PAQs to AhR ligand activity in atmospheric samples was estimated to be significant but not very much (Misaki et al. 2007b). However, considering the contribution of polar fractions to the total AhR ligand activity of road dust and DEPs in the present study, it is probable that several polar compounds such as aliphatic acids, hydroxy-

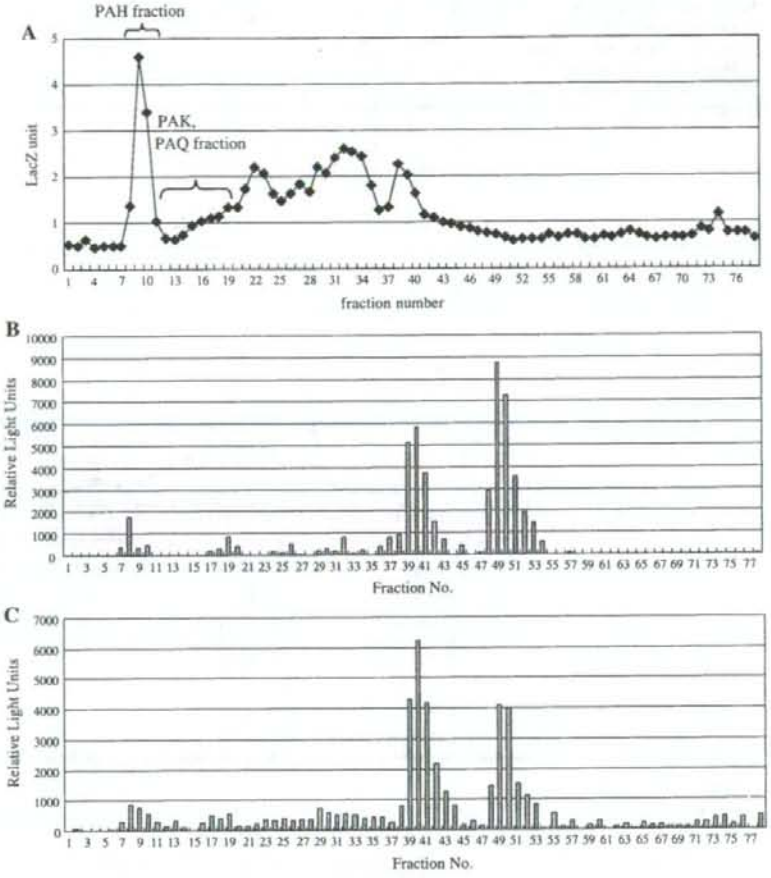

Fig. 4 Second separation of extracts of road dust with a silica gel column and bioassay of fractions. A AhR assay. B ER α assay. C ER β assay

PAHs, polycyclic aromatic carboxaldehydes, polycyclic aromatic carboxylic acids, and polycyclic aromatic anhydrides have significantly potent AhR ligand activity and contribute to the AhR ligand activity of road dust and DEPs (Binková et al. 1998; Casellas et al. 1995; Rogge et al. 1993a, b).

Consequently, AhR ligand activity was confirmed in the extracts of both road dust and DEPS. In the separation of the extracts of both road dust and DEPs with reversed-phase HPLC, it was found that polar fractions contributed to significant AhR ligand activity both in the mouse hepatoma (H1L1) cell system and in the system. Furthermore, the contribution of these polar fractions was higher in DEPs than in road dust. The contribution of the polar region to AhR ligand activity was also observed with the separation of road dust extract by normal-phase HPLC. Additionally, remarkable ER ligand activity was confirmed in the highly polar region separated by normal-phase HPLC. The identification of unknown AhR or ER ligand active compounds and their detailed analysis in the polar region are problems for future study.

Acknowledgments We thank Dr. Charles A. Miller III of the Department of Environmental Health Sciences and the Tulane-Xavier Center for Bioenvironmental Research, Tulane University School of Public Health and Tropical Medicine, New Orleans, Louisiana, for kindly supplying us with the YCM3 strain. We acknowledge the Shiga National Highway Construction Work Office, Kinki Regional Construction Agency, Ministry of Construction, and Ritto Management Office, Nagoya Management Agency, Japan Highway Public Corp., for their cooperation in collection of road dust; Dr. Yoshihisa Shimizu, Research Center for Environmental Quality Management, Kyoto University, for kindly allowing us to use the ASE instrument; and Dr. Ryoichi Kizu, Faculty of Pharmaceutical Sciences, Doshisha Woman's College of Liberal Arts, Kyoto, for kindly providing us with diesel particulates. We also thank Hirofumi Kawami and Tota Tanaka, Research Center for Environmental Quality Management, Kyoto University, and Dr. Byung-Cheol Lee, Department of Environment Research, Korea Institute of Construction Technology, for

Table 1 Retention times of representative PACs in normal-phase HPLC

Retention time	Compound
6–8 min	Naphthalene
	Anthracene
8–11 min	Indeno[1,2,3-*c*,*d*]pyrene
	Pyrene
	Benzo[*a*]pyrene
	Benzo[*k*]fluoranthene
	Dibenz[*a*,*h*]anthracene
	Triphenylene
	Benz[*a*]anthracene
	Chrysene
11–19 min	7,12-Benz[*a*]anthracenequinone
	Benzo[*b*]fluoranthene
	1-Pyrenecarboxilic acid
	1-Pyrenecarboxaldehyde
	5,12-Naphthacenequinone
	Anthraquinone
	11*H*-Benzo[*a*]fluorene-11-one
	6*H*-Benzo[*cd*]pyrene-6-one
	11*H*-Benzo[*b*]fluorene-11-one
	Acridine
	Phenalenone
31 min	1-Hydroxypyrene

their assistance. This work was supported in part by Grants-in-Aid for Scientific Research (13027245, 16201012) from the Japanese Ministry of Education, Science, Sports and Culture.

References

Adachi J, Mori Y, Matsui S, Takigami H, Fujino J, Kitagawa H, Miller III CA, Kato T, Saeki K, Matsuda T (2001) Indirubin and indigo are potent aryl hydrocarbon receptor ligands present in human urine. J Biol Chem 276:31475–31478

Alsberg T, Strandell M, Westerholm R, Stenberg U (1985) Fractionation and chemical analysis of gasoline exhaust particulate extracts in connection with biological testing. Environ Int 11:249–257

Binková B, Lenícek J, Beneš I, Vindová P, Gajdoš O, Fried M, Šrám RJ (1998) Genotoxicity of coke-oven and urban air particulate matter in in vitro acellular assays coupled with ^{32}P-postlabeling and HPLC analysis of DNA adducts. Mutat Res 414:77–94

Bols NC, Schirmer K, Joyce EM, Dixon DG, Greenberg BM, Whyte JJ (1999) Ability of polycyclic hydrocarbons to induce 7-ethoxyresorfin-o-deethylase activity in a trout liver cell line. Ecotoxicol Environ Saf 44:118–128

Burczynski ME, Penning (2000) Genotoxic polycyclic aromatic hydrocarbon ortho-quinones generated by aldo-keto reductases induce CYP1A1 via nuclear translocation of the aryl hydrocarbon receptor. Cancer Res 60:908–915

Casellas M, Fernandez P, Bayona JM, Solanas AM (1995) Bioassay-directed chemical analysis of genotoxic components in urban airborne particulate matter from Barcelona (Spain). Chemosphere 30:725–740

Choi J, Oris JT (2003) Assessment of the toxicity of anthracene photo-modification products using the topminnow (Poeciliopsis lucida) hepatoma cell line (PLHC-1). Aquat Toxicol 65:243–251

Chou P-H, Matsui S, Matsuda T (2006) Detection and identification of dyes showing AhR-binding affinity in treated sewage effluents. Water Sci Technol 53(11):35–42

Chou P-H, Matsui S, Misaki K, Matsuda T (2007) Isolation and identification of xenobiotic aryl hydrocarbon receptor ligands in dyeing wastewater. Environ Sci Technol 41:652–657

Clemons JH, Allan IM, Marvin CH, Wu Z, McCarry BE, Bryant DW, Zacharewski TR (1998) Evidence of estrogen- and TCDD-like activities in crude and fractionated extracts of PM_{10} air

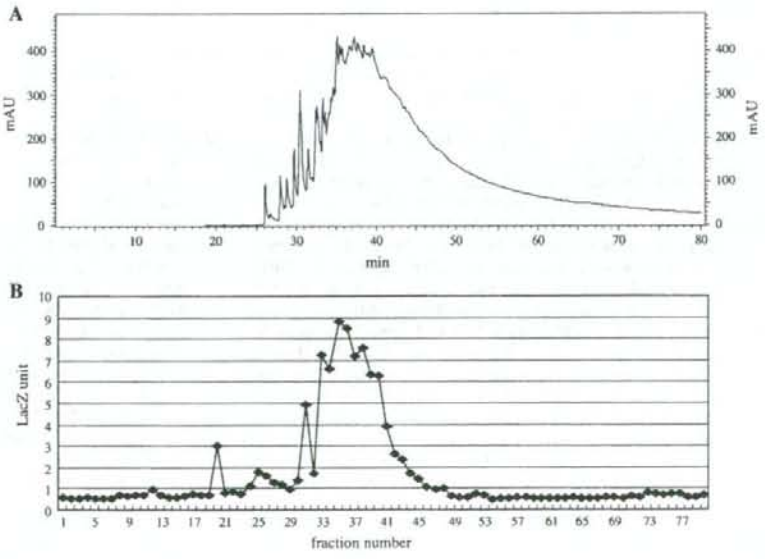

Fig. 5 Third separation with ODS column of fraction 9 in separation with silica gel column and AhR assay for fractions. A UV absorption with 254 nm. B AhR assay

particulate material using in vitro gene expression assays. Environ Sci Technol 32:1853–1860
Colborn T (2004) Endocrine disruption overview: Are males at risk? Adv Exp Med Biol 545:189–201
Crepineau C, Rychen G, Feidt C, Le Roux Y, Lichtfouse E, Laurent F (2003) Contamination of pastures by polycyclic aromatic hydrocarbons (PAHs) in the vicinity of a highway. J Agr Food Chem 51:4841–4845
Denison M, Brouwer A, Clark G (1998) U.S. patent 5,854,010
Denison MS, Pandini A, Nagy SR, Baldwin EP, Bonati L (2002) Ligand binding and activation of the Ah receptor. Chem-Biol Interact 141:3–24
Durant JL, Busby WF Jr, Lafleur AL, Penman BW, Crespi CL (1996) Human cell mutagenicity of oxygenated, nitrated and unsubstituted polycyclic aromatic hydrocarbons associated with urban aerosols. Mutat Res 371:123–157
Fernandez P, Bayona JM (1992) Use of off-line gel permeation chromatography-normal-phase liquid chromatography for the determination of polycyclic aromatic compounds in environmental samples and standard reference materials (air particulate matter and marine sediment). J Chromatogr 625:141–149
Giesy JP, Hilsherova K, Jones PD, Kannan K, Machala M (2002) Cell bioassays for detection of aryl hydrocarbon (AhR) and estrogen receptor (ER) mediated activity in environmental samples. Mar Poll Bull 45:3–16
Hannigan MP, Cass GR, Penman BW, Crespi CL, Lafleur AL, Busby WF Jr, Thilly WG, Simoneit BRT (1998) Bioassay-directed chemical analysis of Los Angeles airborne particulate matter using a human cell mutagenicity assay. Environ Sci Technol 32:3502–3514
Hirose T, Morito K, Kizu R, Toriba A, Hayakawa K, Ogawa S, Inoue S., Muramatsu M, Masamune Y (2001) Estrogenic/antiestrogenic activities of benzo[a]pyrene monohydroxy derivatives. J Health Sci 47:552–558
IARC (1983) Polynuclear aromatic compounds. Part 1. Chemical, environmental and experimental data. IARC Monographs on the Evaluation of the Carcinogenic Risk of Chemicals to Humans. Vol. 32. IARC, Lyon, France
Iida M, Oguri H (2003) Japan patent 2003180393
Jones JM, Anderson JW (1999) Relative potencies of PAHs and PCBs based on the response of human cells. Environ Toxicol Pharmacol 7:19–26
Kamiya M, Toriba A, Onoda Y, Kizu R, Hayakawa K (2005) Evaluation of estrogenic activities of hydroxylated polycyclic aromatic hydrocarbons in cigarette smoke condensate. Food Chem Toxicol 43:1017–1027
Kannan K, Villneuve DL, Yamashita N, Imagawa T, Hashimoto S, Miyazaki A, Giesy JP (2000) Vertical profile of dioxin-like and estrogenic activities associated with a sediment core from Tokyo Bay, Japan. Environ Sci Technol 34:3568–3573
Kawanishi M, Takamura-Enya T, Ermawati R, Shimohara C, Sakamoto M, Matsukawa K, Matsuda T, Murahashi T, Matsui S, Wakabayashi K, Watanabe T, Tashiro Y, Yagi T (2004) Detection of genistein as an estrogenic contaminant of river water in Osaka. Environ Sci Technol 38:6424–6429
Kitamura S, Kato T, Iida M, Jinno N, Suzuki T, Ohta S, Fujimoto N, Hanada H, Kashiwagi K, Kashiwagi A (2005) Anti-thyroid hormonal activity of tetrabromobisphenol A, a flame retardant, and related compounds: affinity to the mammalian thyroid hormone receptor, and effect on tadpole metamorphosis. Life Sci 76:1589–1601
Kizu R, Okamura K, Toriba A, Kakishima H, Mizokami A, Burnstein KL, Hayakawa K (2003) A role of aryl hydrocarbon receptor in the antiandrogenic effects of polycyclic aromatic hydrocarbons in LNCaP human prostate carcinoma cells. Arch Toxicol 77:335–343
Kojima H, Iida M, Katsura E, Kanetoshi A, Hori Y, Kobayashi K (2003) Effects of a diphenyl ether-type herbicide, chlornitrofen, and its amino derivative on androgen and estrogen receptor activities. Environ Health Perspect 111:497–502
Lee B-C, Matsui S, Shimizu Y, Matsuda T (2005a) Characterization of the first flush in storm water runoff from an urban roadway. Environ Technol 26:773–782
Lee B-C, Shimizu Y, Matsuda T, Matsui S (2005b) Characterization of polycyclic aromatic hydrocarbons (PAHs) in different size fractions in deposited road particles (DRPs) from Lake Biwa area, Japan. Environ Sci Technol 39:7402–7409
Lee B-C, Matsui S, Shimizu Y, Matsuda T, Tanaka Y (2005c) A new installation for road runoff: up-flow filtration by porous polypropylene media. Water Sci Technol 52(12):225–232
Letzel T, Pöshl U, Wissiack R, Rosenberg E, Grasserbauer M, Niessner R (2001) Phenyl-modified reversed-phase liquid chromatography coupled ionization mass spectrometry: a universal method for the analysis of partially oxidized aromatic hydrocarbons. Anal Chem 73:1634–1645
Machala M, Vondráček J, Bláha L, Ciganek M, Neča J (2001a) Aryl hydrocarbon receptor-mediated activity of mutagenic polycyclic aromatic hydrocarbons determined using in vitro reporter gene assay. Mutat Res 497:49–62
Machala M, Ciganek M, Bláha L, Minksová K, Vondráček J (2001b) Aryl hydrocarbon receptor-mediated and estrogenic activities of oxygenated polycyclic aromatic hydrocarbons and azaarenes originally identified in extracts of river sediments. Environ Toxicol Chem 20:2736–2743
Matsumoto H, Kashimoto T (1986) Embryotoxicity of organic extracts from airborne particulates in ambient air in the chicken embryo. Arch Environ Contam Toxicol 15:447–452
Mcdonald JD, Barr EB, White RK, Chow JC, Schauer JJ, Zielinska B, Grosjean E (2004) Generation and characterization of four dilutions of diesel engine exhaust for a subchronic inhalation study. Environ Sci Technol 38:2513–2522
Miller CA III (1999) A human aryl hydrocarbon receptor signaling pathway constructed in yeast displays additive responses to ligand mixtures. Toxicol Appl Pharmacol 160:297–303
Misaki K, Matsui S, Matsuda T (2007a) Metabolic enzyme induction by HepG2 cells exposed to oxygenated and nonoxygenated polycyclic aromatic hydrocarbons. Chem Res Toxicol 20:277–283
Misaki K, Kawami H, Tanaka T, Handa Y, Nakamura M, Matsui S, Matsuda T (2007b) Aryl hydrocarbon receptor ligand activity of polycyclic aromatic ketones and polycyclic aromatic quinones. Environ Toxicol Chem 26:1370–1379
Moore MN, Livingstone DR, Widdows J (1989) Hydrocarbons in marine mollusks: biological effects and ecological consequences. In: Varanasi U (ed) Metabolism of polycyclic aromatic hydrocarbons in the aquatic environment. CRC Press, Boca Raton, FL, pp 291–328
Nikolaou K, Masclet P, Mouvier G. (1984) Sources and chemical reactivity of polynuclear aromatic hydrocarbons in the atmosphere—a critical review. Sci Total Environ 32:103–132
Ohtake F, Takeyama K, Matsumoto T, Kitagawa H, Yamamoto Y, Nohara K, Tohyama C, Krust A, Mimura J, Chambon P, Yanagisawa J, Fujii-Kuriyama Y, Kato S (2003) Modulation of oestrogen receptor signalling by association with the activated dioxin receptor. Nature 423:545–550
Ohtake F, Baba A, Takada I, Okada M, Iwasaki K, Miki H, Takahashi S, Kouzmenko A, Nohara K, Chiba T, Fujii-Kuriyama Y, Kato S (2007) Dioxin receptor is a ligand-dependent E3 ubiquitin ligase. Nature 446:562–566
Okamura K, Kizu R, Toriba A, Murahashi T, Mizokami A, Burnstein KL, Klinge CM, Hayakawa K (2004) Antiandrogenic activity of extracts of diesel exhaust particles emmited from diesel-engine

truck under different engine loads and speeds. Toxicology 195:243–254

Pedersen DU, Durant JL, Taghizadeh K, Hemond HF, Lafleur AL, Cass GR (2005) Human cell mutagens in respirable airborne particles from the northeastern United States. 2. Quantification of mutagens and other organic compounds. Environ Sci Technol 39:9547–9560

Rogge WF, Hildemann LM, Mazurek MA, Cass GR (1993a) Sources of fine organic aerosol. 2. Noncatalyst and catalyst-equipped automobiles and heavy-duty diesel trucks. Environ Sci Technol 27:636–651

Rogge WF, Hildemann LM, Mazurek MA, Cass GR (1993b) Sources of fine organic aerosol. 3. Road dust, tire debris, and organometallic brakes lining dust: Roads as sources and sinks. Environ Sci Technol 27:1892–1904

Schmidt JV, Bradfield CA (1996) Ah receptor signaling pathways. Annu Rev Cell Dev Bioll 12:55–89

Till M, Riebniger D, Schmitz H-J, Schrenk D (1999) Potency of various polycyclic aromatic hydrocarbons as inducers of CYP1A1 in rat hepatocyte cultures. Chem-Biol Interact 117:135–150

Tsukue N, Toda N, Tsubone H, Sagai M, Jin WZ, Watanabe G, Taya K, Birumachi J, Suzuki AK (2001) Diesel exhaust (DE) affects the regulation of testicular function in male fischer 344 rats. J Toxicol Environ Health A 63:115–126

Tsukue N, Yoshida S, Sugawara I, Takeda K (2004) Effect of diesel exhaust on development of fetal reproductive function in ICR female mice. J Health Sci 50:174–180

van Lipzig MMH, Vermeulen ME, Gusinu R, Legler J, Frank H, Seidel A, Meerman JHN (2005) Formation of estrogenic metabolites of benzo[a]pyrene and chrysene by cytochrome P450 activity and their combined and supra-maximal estrogenic activity. Environ Toxicol Pharmacol 19:41–55

Vos JG, Dybing E, Greim HA, Ladefoged O, Lambre C, Terazona JV, Brandt I, Vethaak AD (2000) Health effects of endocrine-disrupting chemicals on wildlife, with special reference to the European situation. Crit Rev Toxicol 30:71–133

Watanabe N, Oonuki Y (1999) Inhalation of diesel engine exhaust affects spermatogenesis in growing male rats. Environ Health Perspect 107:539–544

Wells PG, Kim PM, Laposa RR, Nicol CJ, Parman T, Winn LM (1997) Oxidative damage in chemical teratogenesis. Mutat Res 396:65–78

Yoshida S, Sagai M, Oshio S, Umeda T, Ihara T, Sugamata M, Sugawara I, Takeda K (1999) Exposure to diesel exhaust affects the male reproductive system of mice. Int J Androl 22:307–315

Ziccardi MH, Gardner IA, Denison MS (2002) Application of the luciferase recombinant cell culture bioassay system for the analysis of polycyclic aromatic hydrocarbons. Environ Toxicol Chem 21:2027–2033

Mutation Research xxx (2009) xxx–xxx

Contents lists available at ScienceDirect

Mutation Research/Fundamental and Molecular Mechanisms of Mutagenesis

journal homepage: www.elsevier.com/locate/molmut
Community address: www.elsevier.com/locate/mutres

Role of Parp-1 in suppressing spontaneous deletion mutation in the liver and brain of mice at adolescence and advanced age

Atsushi Shibata[a,b,c], Daisuke Maeda[a,b], Hideki Ogino[a,b], Masahiro Tsutsumi[d], Takehiko Nohmi[e], Hitoshi Nakagama[a], Takashi Sugimura[a], Hirobumi Teraoka[c], Mitsuko Masutani[a,b,*]

[a] Biochemistry Division, National Cancer Center Research Institute, Chuo-ku, Tokyo 104-0045, Japan
[b] ADP-ribosylation in Oncology Project, National Cancer Center Research Institute, Chuo-ku, Tokyo 104-0045, Japan
[c] Medical Research Institute, Tokyo Medical and Dental University, Chiyoda-ku, Tokyo 101-0062, Japan
[d] Pathology, Saiseikai Chuwa Hospital, Sakurai-City, Nara 633-0054, Japan
[e] Division of Genetics and Mutagenesis, National Institute of Health Sciences, Setagaya-ku, Tokyo 158-8501, Japan

ARTICLE INFO

Article history:
Received 16 August 2008
Received in revised form 30 January 2009
Accepted 4 February 2009
Available online xxx

Keywords:
Parp-1
Mutation
Deletion
gpt delta
Aging

ABSTRACT

Poly(ADP-ribose) polymerase-1 knockout (*Parp-1*$^{-/-}$) mice show increased frequency of spontaneous liver tumors compared to wild-type mice after aging. To understand the impact of *Parp-1* deficiency on mutations during aging, in this study, we analyzed spontaneous mutations in *Parp-1*$^{-/-}$ aged mice. *Parp-1*$^{-/-}$ mice showed tendencies of higher mutation frequencies of the *red/gam* genes at 18 months of age, compared to *Parp-1*$^{+/+}$ mice, in the liver and brain. Complex-type deletions, accompanying small insertion were observed only in *Parp-1*$^{-/-}$ mice in the liver and brain. Further analysis in the liver showed that the frequency of single base deletion mutations at non-repeat or short repeat sequences was 5.8-fold higher in *Parp-1*$^{-/-}$ than in *Parp-1*$^{+/+}$ mice ($p < 0.05$). A 3.2-fold higher tendency of the deletion frequency of two bases or more was observed in *Parp-1*$^{-/-}$ mice compared to *Parp-1*$^{+/+}$ mice ($p = 0.084$). These results support the model that *Parp-1* is involved in suppressing imprecise repair of endogenous DNA damage leading to deletion mutation during aging. The mutation frequencies of the *gpt* gene in the brain were found to be 3-fold lower in *Parp-1*$^{-/-}$ than in *Parp-1*$^{+/+}$ mice at 4 months of age ($p < 0.01$), implying that Parp-1 may be positively involved in imprecise DNA repair in the brain. On the other hand, the frequencies of *gpt* mutation showed an increase at 18 months of age in the *Parp-1*$^{-/-}$ ($p < 0.05$) but not in *Parp-1*$^{+/+}$ brains, suggesting that *Parp-1* deficiency causes an increase of point mutations in the brain by aging.

1. Introduction

Poly(ADP-ribose) polymerase-1 (Parp-1) facilitates DNA strand break repair by binding to the end of DNA strand breaks and catalyzing transfer of ADP-ribose residues from NAD to itself and other nuclear proteins, including XRCC1 (X-ray cross-complementing factor 1) [1], WRN (Werner's syndrome protein) [2,3] and Ku70/80 [4,5]. PolyADP-ribosylation results in recruitment of DNA repair proteins to DNA damage sites [6,7]. Accumulating studies have indicated that Parp-1 is involved in base excision repair (BER) and single strand break (SSB) repair by interacting with XRCC1 through poly(ADP-ribose) residues, as well as DNA polymerase β [8] and DNA ligase IIIα [9] using the BRCT domain in Parp-1. We previously demonstrated that *Parp-1*$^{-/-}$ mice show higher susceptibility to carcinogenesis induced by alkylating agents such as *N*-nitrosobis(2-hydroxypropyl)amine (BHP) [10] and azoxymethane [11] but not with 4-nitroquinoline 1-oxide [12]. *Parp-1*$^{-/-}$ mice develop normally, and spontaneous tumor incidences in all organs are not elevated at least until 9 months old [11]. However, the incidences of hepatocellular adenomas and carcinomas in *Parp-1*$^{-/-}$ mice are increased at 18–24 months old compared to *Parp-1*$^{+/+}$ mice [13]. *Parp-1*$^{-/-}$*p53*$^{-/-}$ mice also show spontaneous medulloblastomas in *p53* knockout (*p53*$^{-/-}$) mice at a higher incidence compared to *Parp-1*$^{+/+}$*p53*$^{-/-}$ mice [14,15].

In wild-type mice, age-related increases of mutant frequencies are observed in the liver, spleen, heart and small intestine, whereas mutant frequencies in the brain and germ cells are only slightly increased [16–18]. Age-related increases in genome rearrangement as well as point mutations are reported in the liver but not observed in the brain [19]. Therefore, the effects of aging on spontaneous mutation frequency might be different among tissues.

To analyze the impact of aging on spontaneous mutant frequency and its spectra in *Parp-1*$^{-/-}$ mice, we performed mutation analysis in *Parp-1*$^{-/-}$ mice at advanced age using progeny of

* Corresponding author at: Biochemistry Division, National Cancer Center Research Institute, 5-1-1, Chuo-ku, Tokyo 104-0045, Japan. Tel.: +81 3 3542 2511; fax: +81 3 3542 2530.
E-mail address: mmasutan@ncc.go.jp (M. Masutani).

0027-5107/$ – see front matter © 2009 Elsevier B.V. All rights reserved.
doi:10.1016/j.mrfmmm.2009.02.001

intercross with *gpt* delta transgenic mice harboring about 80 copies of tandemly integrated lambda EG10 DNA as a transgene [20,21]. The rescued phage was analyzed by the Spi⁻ (sensitive to P2 interference) assay, which preferentially detects deletion mutations in the *red/gam* genes. The deletion mutations of a single base to approximately 10 kb or several copies of EG10 DNA could be detected. The *gpt* assay detects point mutations in the guanine phosphoribosyl transferase (*gpt*) gene. The spontaneous mutant frequency of the *gpt* gene in the liver of mice is around $2–6 \times 10^{-6}$ [23] in tissues including the liver and brain [24]. The frequency of mutation in the *red/gam* genes in the liver of mice is also reported to be around $1–5 \times 10^{-6}$ [23,24].

Analysis of deletion mutation with a Spi⁻ assay using *gpt* delta transgenic mice has been shown to be useful in detecting deletion mutations after treatment with various types of chemicals or irradiation with γ-rays or heavy ions [23,25–26].

The results in this study suggest that Parp-1 suppresses spontaneous deletion mutations, especially at non-repeat or short repeat sequences in the liver and brain during aging. Complex-type deletions accompanying small insertion and microhomology at deletion junctions observed in *Parp-1*$^{-/-}$ livers and brains are also discussed. Additionally, we observed that the mutant frequencies of the *gpt* gene in the brains were found to be 3-fold lower in *Parp-1*$^{-/-}$ than in *Parp-1*$^{+/+}$ mice at 4 months of age but increased in *Parp-1*$^{-/-}$ mice to the level of *Parp-1*$^{+/+}$ mice at 18 months of age.

2. Materials and methods

2.1. Genomic DNA extraction and rescue of the transgene

Parp-1$^{-/-}$/*gpt* delta and *Parp-1*$^{+/+}$/*gpt* delta animals were previously established by intercrossing *Parp-1*$^{+/-}$/*gpt* delta mice [20]. The mice possess mixed genetic background of C57BL/6, ICR and 129Sv. Male *Parp-1*$^{-/-}$ and *Parp-1*$^{+/+}$ mice were fed a basal diet (CE-2, Clea Japan), and these mice were anaesthetized and sacrificed at the ages of 4 months ($n = 5$ for each genotype) and 18 months ($n = 6$ (*Parp-1*$^{-/-}$) and $n = 4$ (*Parp-1*$^{+/+}$)). The livers and brains were immediately frozen in liquid nitrogen, and stored at −80 °C until DNA extraction. Genomic DNA was extracted by a RecoverEase DNA isolation kit (Stratagene). Two out of six *Parp-1*$^{-/-}$ mice (mouse ID, G60 and G94) of 18 months of age harbored tumors in the liver, and genomic DNA was extracted from areas containing no tumors. A lambda phage *in vitro* packaging reaction was performed with Transpack Packaging Extract (Stratagene). Part of the tissues were also fixed with formalin solution, routinely processed and sections were stained with hematoxyline-eosine. The experimental protocol was approved by the Ethics Review Committee for Animal Experimentation of the National Cancer Center Research Institute.

2.2. Spi⁻ assay

A Spi⁻ assay [21] was carried out with a modification as described previously [27]. The frequencies of background mutants were less than 10^{-8} in the Spi⁻ assay and were negligible [28]. The data for Spi⁻ mutant frequencies were therefore presented without subtracting the background mutant frequencies. To narrow down the deleted region, the structure of each mutation was analyzed by a Southern blot hybridization method that uses oligonucleotide DNA probes [29]. DNA sequencing of the mutated region was performed with a CEQ™ DTCS Quick Start Kit (Beckman Coulter).

2.3. gpt assay

The *gpt* assay was performed as described previously [21]. Briefly, the phages rescued from genomic DNA were transfected into *E. coli* YG6020 expressing Cre recombinase. Infected cells were cultured at 37 °C on plates containing chloramphenicol (Cm) and 6-thioguanine (6-TG) for 3 days until 6-TG resistant colonies appeared. To confirm the 6-TG resistant phenotype, colonies were restreaked on plates containing Cm and 6-TG. A 739 bp DNA fragment encompassing the *gpt* gene was amplified by PCR [30]. DNA sequencing of the target 456 bp in the *gpt* gene was performed with a CEQ™ DTCS Quick Start Kit (Beckman Coulter).

2.4. Statistical analysis

The statistical significance of differences in mutant or mutation frequencies between the two groups was analyzed by using the Mann–Whitney *U* test. When *p* value is less than 0.05, the difference was considered significant. Because the individual differences in mutant frequency became larger at advanced ages, "tendency of ≥1.5 fold increase or reduction" in the mutant frequency is also mentioned with *p* value in the text, when *p* value is equal to or larger than 0.05.

3. Results

3.1. Analysis of spontaneous mutant frequency of the red/gam genes and the gpt genes in the livers of Parp-1$^{-/-}$ mice at 4 and 18 months of age

There was no difference in the mutant frequencies of the *red/gam* genes in the liver between *Parp-1*$^{-/-}$ and *Parp-1*$^{+/+}$ mice at 4 months of age. The liver of *Parp-1*$^{-/-}$ mice at 18 months of age showed a 1.7-fold higher tendency of the *red/gam* mutant frequencies than those in *Parp-1*$^{+/+}$ mice ($p = 0.34$, Fig. 1A). The tendency of age-dependent 1.5-fold increase in mutant frequency was observed in *Parp-1*$^{-/-}$ but not in *Parp-1*$^{+/+}$ mice.

On the other hand, in the case of the *gpt* gene (Fig. 1B), in which point mutations are mostly detected, the mutant frequencies in *Parp-1*$^{+/+}$ mice showed a higher elevation at 18 months than that at 4 months ($p = 0.037$). In *Parp-1*$^{-/-}$ mice, a tendency of higher mutant frequency was noticed at 18 months compared to that at 4 months ($p = 0.14$). There was no significant difference in the mutant frequency of *gpt* gene between *Parp-1*$^{-/-}$ and *Parp-1*$^{+/+}$ mice at either 4 or 18 months (Fig. 1B).

3.2. Structural analysis of deletion mutations in the red/gam genes of Parp-1$^{-/-}$ mice at 18 months of age

The mutations in the *red/gam* genes could be categorized into deletion, base substitution and single base insertion. As shown in Fig. 1C, deletion mutation frequencies in the liver of *Parp-1*$^{-/-}$ mice showed a tendency of 1.7-fold increase compared to those in *Parp-1*$^{+/+}$ mice ($p = 0.20$). The deletion mutations could be classified into single base deletion and deletion of two bases or more (Fig. 1C). Fig. 1D shows the distribution of single base deletions of the *gam* gene in the liver of *Parp-1*$^{-/-}$ and *Parp-1*$^{+/+}$ mice at 18 months of age. Single nucleotide repeats, –AAAAA– at 227–231, –AAAAAA– at 295–300 and –GGGG– at 286–289, are known as hot spots of single base deletions in the *gam* gene of wild-type mice [28]. The frequency of single base deletions at hot spots, namely at 4–6 bp mononucleotide repeats was not increased in *Parp-1*$^{-/-}$ mice compared to *Parp-1*$^{+/+}$ mice (Fig. 1C). In contrast, the frequency of single base deletions at non-repeat sequences or short repeats of 2–3 bp mononucleotides showed a 5.8-fold increase in *Parp-1*$^{-/-}$ mice ($p = 0.031$, Fig. 1C). The single base deletions at non-repeat sequences were only observed in *Parp-1*$^{-/-}$ mice at a frequency of 4.3×10^{-7} and showed a higher frequency than that in *Parp-1*$^{+/+}$ mice ($p = 0.023$). The specific deletion mutation frequencies of two bases or more in the liver showed a 3.2-fold (Fig. 1C) higher tendency in *Parp-1*$^{-/-}$ mice than those in *Parp-1*$^{+/+}$ mice, although there was no statistical significance ($p = 0.084$). Deletions of both 2 bp–1 kb and deletions larger than 1 kb were observed in the liver of *Parp-1*$^{-/-}$ mice, whereas all three mutants in *Parp-1*$^{+/+}$ mice (Table 1) had deletions larger than 1 kb (data not shown).

The deletion mutations of two bases or more were also categorized into those that occurred at non-repeat and short repeat sequences of mononucleotides. Frequencies of deletion mutations of two bases or more at non-repeat and short repeats of mononucleotides showed a higher tendency in *Parp-1*$^{-/-}$ than *Parp-1*$^{+/+}$ mice ($p = 0.28$) at 18 months old (Fig. 1C). There was no deletion mutation of two bases or more that occurred on a mononucleotide repeat larger than 4 bp in both genotypes.

We further categorized deletion mutations of two bases or more into simple or complex types (Table 1). Complex-type deletions were defined as accompanying small insertions or recombination with deletions [20]. Complex-type deletions were found in

Please cite this article in press as: A. Shibata, et al., Role of Parp-1 in suppressing spontaneous deletion mutation in the liver and brain of mice at adolescence and advanced age, Mutat. Res.: Fundam. Mol. Mech. Mutagen. (2009), doi:10.1016/j.mrfmmm.2009.02.001

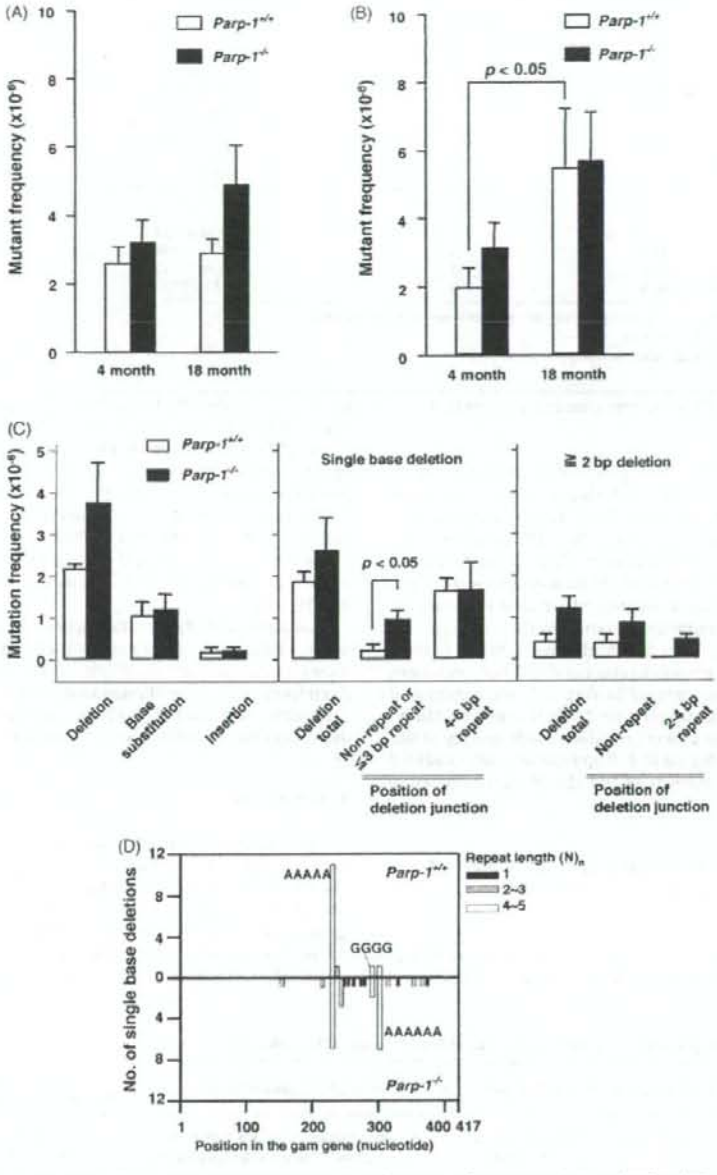

Fig. 1. Spontaneous mutant frequencies of the *red/gam* and *gpt* genes in the liver of *Parp-1*$^{-/-}$ and *Parp-1*$^{+/+}$ mice at 4 and 18 months of age. (A) Spontaneous mutant frequencies of the *red/gam* genes in the livers. (B) Spontaneous mutant frequencies in the *gpt* genes of the livers. Error bars represent standard error values. (C) Effect of *Parp-1* deficiency on the mutation spectrum of the *red/gam* genes in the liver at 18 months of age. Specific mutation frequencies in the *red/gam* genes of the liver are shown. Mean values and standard error values are presented for *Parp-1*$^{-/-}$ and *Parp-1*$^{+/+}$ mice ($n = 6$ and 4, respectively). (D) Distribution of single base deletion mutations in the *gam* gene of the livers at 18 months of age. Single base deletions were observed on non-repeat, or 2–3 base repeats, or 4–6 base repeats as indicated in the figure as repeat length $(N)_n$ of 1, 2, 4–6, respectively.

Parp-1$^{-/-}$ mice, but not in *Parp-1*$^{+/+}$ mice in the liver at 18 months old. As shown in Table 1, the frequencies of complex-type deletions in *Parp-1*$^{-/-}$ mice showed a higher tendency than those in *Parp-1*$^{+/+}$ mice, although it is not statistically significant ($p = 0.224$). The structures of complex-type mutations of *Parp-1*$^{-/-}$ mice observed at 18 months of age are shown in Table 2. Two complex-type deletions observed in *Parp-1*$^{-/-}$ mice accompanied both small insertions and microhomologous sequences at deletion junctions (Table 2). It is of note that complementary nucleotides AAA (G61-1-3) or TT (G93-2-3) (marked with upper lines in Table 2) are present at the 5′ position to these microhomologous deletion junctions in each case.

Please cite this article in press as: A. Shibata, et al., Role of Parp-1 in suppressing spontaneous deletion mutation in the liver and brain of mice at adolescence and advanced age, Mutat. Res.: Fundam. Mol. Mech. Mutagen. (2009), doi:10.1016/j.mrfmmm.2009.02.001

Table 1
Spectrum of the mutations of two bases or more in the *red/gam* genes in the liver and brain of *Parp-1*$^{-/-}$ mice at 18 months old.

Tissue	Deletion	*Parp-1*$^{+/+}$		*Parp-1*$^{-/-}$	
		Mutation frequency ($\times 10^{-6}$)	No. of mutants (MEJ/Non-MEJ)	Mutation frequency ($\times 10^{-6}$)	No. of mutants (MEJ/Non-MEJ)
Liver	Simple	0.34 ± 0.21	3 (2/1)	0.96 ± 0.27	13 (6/7)
	Complex	<0.16	0	0.13 ± 0.08	2 (2/0)
	with small insertion[a]	<0.16	0	0.13 ± 0.08	2 (2/0)
	with recombination	<0.16	0	<0.13	0
Brain	Simple	0.15 ± 0.15	1 (0/1)	0.32 ± 0.14	3 (2/1)
	Complex	<0.18	0	0.32 ± 0.14	3 (1/1)[b]
	with small insertion	<0.18	0	0.19 ± 0.12	2 (1/1)
	with recombination	<0.18	0	0.12 ± 0.12	1

MEJ; microhomology-mediated end joining. Non-MEJ; non-microhomology-mediated end joining.
[a] Small insertion represents 4–9 bp insertion.
[b] One of the mutants could not be classified into MEJ or non-MEJ type.

3.3. Mutation frequencies of the red/gam gene in the brains at 4 and 18 months of age

Parp-1$^{-/-}$ mice showed 1.5-fold higher mutant frequencies compared to *Parp-1*$^{+/+}$ mice ($p = 0.047$) in the brains at 4 months of age (Fig. 2A). The brains of *Parp-1*$^{-/-}$ mice showed a 2.2-fold higher tendency of mutant frequencies than those in *Parp-1*$^{+/+}$ mice ($p = 0.088$) at 18 months of age (Fig. 2A). The tendency of age-dependent slight increase in the mutant frequency in the brain was observed in *Parp-1*$^{-/-}$ but not in *Parp-1*$^{+/+}$ mice, as mentioned earlier in the case with the liver. Analysis of the mutation spectrum in the brain (Fig. 2C) revealed some differences from that of the livers. In the brain, a tendency of increase in base substitution and deletion mutations of two bases or more was observed in *Parp-1*$^{-/-}$ mice compared to *Parp-1*$^{+/+}$ mice (base substitution: $p = 0.055$, deletion mutation: $p = 0.11$). Different from the cases in the liver, the frequency of single base deletions at non-repeat or 2–3 bp repeats is not increased in the brain of *Parp-1*$^{-/-}$ mice at 18 months of age compared to *Parp-1*$^{+/+}$ mice (Fig. 2C).

3.4. Lower mutation frequencies of the gpt gene in the brains of Parp-1$^{-/-}$ than Parp-1$^{+/+}$ mice at 4 months of age and age-dependent increase

Of note, mutant frequencies of the *gpt* gene in the brains of *Parp-1*$^{-/-}$ mice were lower than those of *Parp-1*$^{+/+}$ mice ($p = 0.009$) at 4 months of age (Fig. 2B). No pathological changes in the brains were observed in *Parp-1*$^{-/-}$ and *Parp-1*$^{+/+}$ mice. Mutation spectra in the brains of *Parp-1*$^{-/-}$ mice showed a lower frequency of G:C to A:T base transition mutations ($p = 0.047$) as well as deletion mutations ($p = 0.034$) compared to *Parp-1*$^{+/+}$ mice at 4 months old (Fig. 2D).

The *gpt* mutant frequency showed an increase at 18 months of age in the *Parp-1*$^{-/-}$ but not in *Parp-1*$^{+/+}$ mice ($p = 0.011$, Fig. 2B). There was no difference in the mutant frequencies of the *gpt* gene in the brain between *Parp-1*$^{-/-}$ and *Parp-1*$^{+/+}$ mice at 18 months of age (Fig. 2B).

Comparison of the mutation spectra between 4 and 18 months of age in *Parp-1*$^{-/-}$ mice suggests a tendency of age-dependent increase in the frequencies of deletion mutations ($p = 0.068$, Fig. 2D). A tendency of increase of point mutation ($p = 0.144$) is also noticed, suggesting that Parp-1 may be involved in suppressing age-dependent introduction of point mutations in the brain.

4. Discussion

Spontaneous *gpt* and *red/gam* mutant frequencies are reported to be around $2–6 \times 10^{-6}$ and $1–5 \times 10^{-6}$, respectively, in *gpt* delta mice of C57BL/6 genetic background [23,24]. In this study, the spontaneous mutation frequencies of *gpt* and *red/gam* mutant frequencies in the liver and the brain of *Parp-1*$^{+/+}$ are both around 2×10^{-6} at 4 months of age and thus consistent with the previous reports. The mutant frequency of the *gpt* gene in the small intestine

Table 2
Junctional sequences of complex-type mutations in the liver and brain of *Parp-1*$^{-/-}$ mice at 18 months old.

Tissue	Mutant ID[a]	Original sequence in lambdaEG10	Junctional sequence of mutation	Deletion/insertion size (nucleotide position in lambdaEG10)
Liver	G61-1-3	5′-GTCATCAAACgcac 3′-CAGTAGTTTGcgtg	tttt**gc**TGGCCCCG-3′ aaaa**CG**ACCGGGGC-5′	20 bp deletion + 4 bp insertion (25021 - 25040)
	G93-2-3	5′-CCGTGGCGTTggaa 3′-GGCACCGCAAcgtt	ataa**GC**GTTCATGG-3′ tatt**CG**CAAGTACC-5′	149 bp deletion + 6 bp insertion (25058 - 25206)
Brain	G61-1-1	5′-TTCATTAGACttat 3′-AAGTAATCTGaata	tagtGAATGCTTTT-3′ atcaCTTACGAAAA-5′	3694 bp deletion + 6 bp insertion (21600 - 25293)
	G94-1-1	5′-TGTCTGCATGgaga 3′-ACAGACGTACctct	aatc**GA**TTTCCCT-3′ ttagCTAAAGGGA-5′	3805 bp deletion + 9 bp insertion (21682 - 25486)
	G93-2-4		acgcGCCCAGCTCT-3′ tgcgCGGGTCGAGA-5′	5′-taagagtcagGCCCAGCTCT-3′ 3′-attctcagtcCGGGTCGAGA-5′ Recombination with unknown sequence

[a] ID; Identification number. Red and blue letters indicate deleted and inserted sequences, respectively. Letters in the box are microhomologous sequences. Upperlines show complementary mononucleotide sequences at 5′ positions of the microhomologous sequences.

Please cite this article in press as: A. Shibata, et al., Role of Parp-1 in suppressing spontaneous deletion mutation in the liver and brain of mice at adolescence and advanced age, Mutat. Res.: Fundam. Mol. Mech. Mutagen. (2009), doi:10.1016/j.mrfmmm.2009.02.001

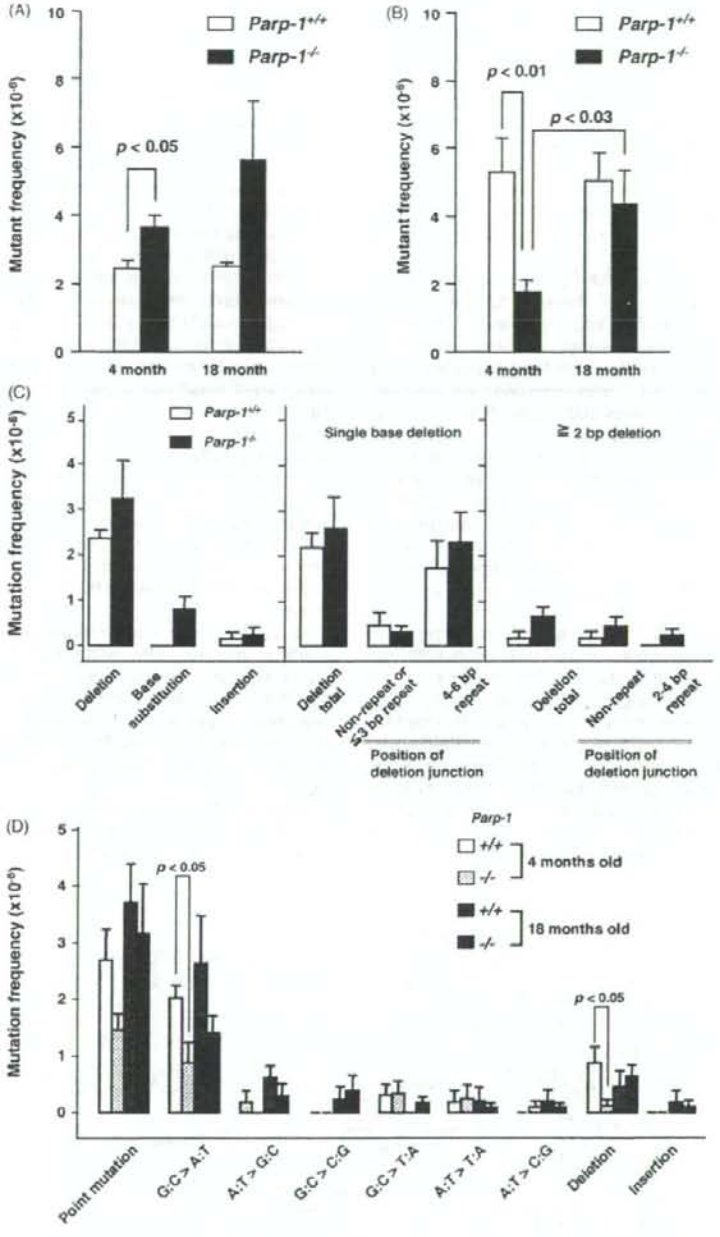

Fig. 2. Spontaneous mutant frequencies of the *red/gam* and *gpt* genes in the brain of *Parp-1*$^{-/-}$ and *Parp-1*$^{+/+}$ mice at 4 and 18 months of age. (A) Spontaneous mutant frequencies of the *red/gam* genes. (B) Spontaneous mutant frequencies in the *gpt* genes. Error bars represent standard error values. (C) Mutation spectra of the *red/gam* genes in the brain of *Parp-1*$^{-/-}$ and *Parp-1*$^{+/+}$ mice at 18 months of age. (D) Mutation spectra of the *gpt* genes in the brain of *Parp-1*$^{-/-}$ and *Parp-1*$^{+/+}$ mice at 4 and 18 months of age.

of *gpt* delta transgenic mice of mixed genetic background of SWR and C57BL/6 is reported to be 2.5×10^{-5} [22], which is higher compared to other reports on *gpt* delta mice [23,24]. This difference could be due to the mouse strain, tissues or other factors. From 4 to 18 months of age, the mutant frequency of the *gpt* gene in *Parp-1*$^{+/+}$ mice increased 2-fold. The mutant frequency of the *lacZ* marker gene in the liver is around 5×10^{-6} at 4–6 months of age and 1.2×10^{-5} at 24–34 months of age in wild-type mice [19]. Therefore age-dependent 2-fold increase in mutant frequency is consistently observed both in the *gpt* and *lacZ* [19] genes. On the other hand, size change mutations in the liver detected by the *lacZ* gene system did not significantly increase before 25–27 months [19] but

Please cite this article in press as: A. Shibata, et al., Role of Parp-1 in suppressing spontaneous deletion mutation in the liver and brain of mice at adolescence and advanced age, Mutat. Res.: Fundam. Mol. Mech. Mutagen. (2009), doi:10.1016/j.mrfmmm.2009.02.001

increased thereafter. Increase of mutant frequency in the *red/gam* gene in *Parp-1*$^{+/+}$ mice at 18 months of age, which detects deletion mutation, was not observed in the liver, being consistent with the results in the *lacZ* gene [19]. In the *lacZ* gene system, the target size is around 3000 bp, whereas that in the *gpt* and *red/gam* gene (Spi$^-$ assay) are around 456 and 417 bp, respectively. The smaller size of the target sequences of the *gpt* and *red/gam* genes could be also responsible for the lower spontaneous mutant frequencies.

In this study, *Parp-1*$^{-/-}$ mice showed a tendency of higher frequencies of spontaneous deletion mutations in the *red/gam* gene, including complex-type deletions in the liver ($p = 0.20$) and brain ($p = 0.29$) at 18 months of age.

The single base deletion mutations at non-repeat or short repeat sequences of the *red/gam* gene showed a 5.8-fold increase ($p = 0.031$) in the liver of *Parp-1*$^{-/-}$ mice compared to *Parp-1*$^{+/+}$ mice at 18 months of age. The frequency of deletion mutations of two bases or more also showed a 3.2-fold higher tendency in the *Parp-1*$^{-/-}$ than in the *Parp-1*$^{+/+}$ liver ($p = 0.084$). We observed complex-type deletions in the livers and brains of *Parp-1*$^{-/-}$ but not in *Parp-1*$^{+/+}$ mice at 18 months old.

8-Oxodeoxyguanosine (8-oxodG) is one outcome of major oxidative DNA damage [31]. The 8-oxodG levels in DNA of the liver, lungs, and small intestine in double knockout mice lacking both 8-oxoguanine DNA glycosylase 1 (*Ogg1*) and Mut Y homologue (*Myh*) genes increased linearly between 4 and 14 months of age [32]. 8-OxodG and SSB, which are expected outcomes of major endogenous DNA damage, are preferentially repaired by BER. Parp-1 is shown to be involved in BER and deletion mutations of single base and larger sizes of deletion as well as complexed-type were increased in *Parp-1*$^{-/-}$ mice after treatment with an alkylating agent, BHP [20]. The frequency of single base deletion mutations at non-repeat or short repeat sequences of the *red/gam* gene also increased 2.9-fold in *Parp-1*$^{-/-}$ mice compared to *Parp-1*$^{+/+}$ mice ($p = 0.043$) in the liver after treatment of the alkylating agent, whereas no difference in the frequency of single base deletion at 4–6 bp of mononucleotide repeats was observed between genotypes [20]. Therefore the spectra of single base deletions in the liver of *Parp-1*$^{-/-}$ mice at advanced age and after treatment with the alkylating agent are similar to each other. Stalled BER in the absence of Parp-1 at a SSB introduced step may further cause deletion mutations after treatment with an alkylating agent [20]. Therefore, there is a possibility that deletion mutation is also caused through BER induced by endogenous DNA damage during aging in *Parp-1*$^{-/-}$ mice. After introduction of SSB during BER, lack of Parp-1 may induce stall or delay in BER and terminal nucleotides may be destabilized and lost under *Parp-1* deficiency by exonuclease activity (Fig. 3). Collision between SSB and replication forks induces double strand breaks (DSBs) [33]. Two SSBs on opposite strands within at least 30 nt could resolve into a DSB [34]. Therefore, an increase of spontaneous DSBs might also be caused by the presence of SSBs during replication fork progression or defective BER under *Parp-1* deficiency.

Deletion mutations including single base deletions may be also produced during imprecise non-homologous end joining (NHEJ). In NHEJ reconstituted systems that utilize DSB substrates, it is shown that deletion or insertion of single bases as well as larger sizes occurs during the NHEJ process [35–37]. In chicken DT-40 cells, Parp-1 negatively regulates the NHEJ process by inhibiting Ku70/Ku80 action, and *Parp-1* deficiency causes an increase of NHEJ frequency [38]. However, DT-40 cells are known to have high HR levels compared to typical mammalian somatic cells. Using mouse embryonic fibroblast or CHO cells, it is demonstrated that Parp-1 competes with Ku for DSB binding and is shown to be involved in a backup pathway of classical NHEJ pathway with DNA ligase III [39]. Therefore, as shown in Fig. 3, during a NHEJ process of DSB, terminal nucleotides may be destabilized in the absence of Parp-1, and resection of bases by the exonuclease may lead to deletion mutation.

It is also notable that the frequency of single base deletions at 4–6 bp mononucleotide repeats did not show a difference between either genotypes in the livers and brains. Single base deletion mutations at 4–6 bp of mononucleotide repeats, namely at run sequences, might be caused by slippage error during DNA replication or repair reaction. The results suggest that Parp-1 is not essential to suppress these slippage type errors induced during aging.

Two complex-type deletions observed in *Parp-1*$^{-/-}$ mice accompanied small insertions as well as microhomologous sequences at deletion junctions, suggesting that these mutations could be

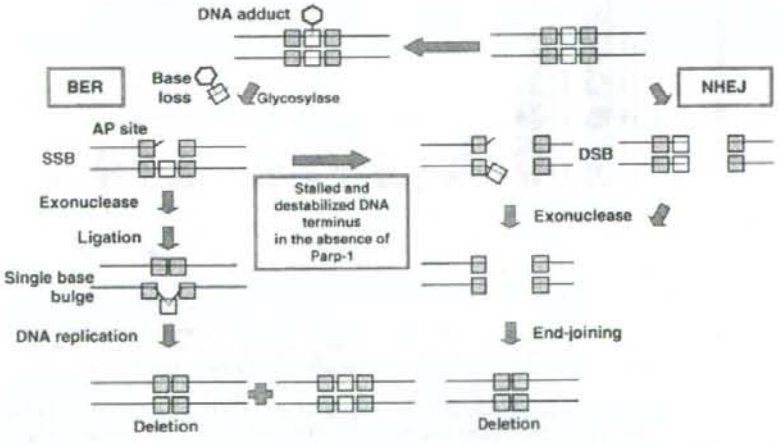

Fig. 3. A model for augmented development of deletion mutation through imprecise BER or NHEJ process in the absence of Parp-1. During BER, after single strand breaks are introduced following damaged base removal, the DNA terminus may be destabilized in the absence of Parp-1. Base loss could occur by the DNA exonuclease activity. When misannealing and ligation occur, the deletion will be fixed by subsequent DNA replication. Stalled BER reaction in the absence of Parp-1 on single strand breaks may also cause DSB and may induce switching to a NHEJ reaction and subsequently base loss will be fixed by end-joining process. During DSB repair process by NHEJ, base loss frequency might be augmented at the destabilized DNA terminus in the absence of Parp-1.

Please cite this article in press as: A. Shibata, et al., Role of Parp-1 in suppressing spontaneous deletion mutation in the liver and brain of mice at adolescence and advanced age, Mutat. Res.: Fundam. Mol. Mech. Mutagen. (2009), doi:10.1016/j.mrfmmm.2009.02.001

caused by insertion of a few nucleotides during microhomologous end-joining (ME])-type reactions. A few complementary bases are present at the 5′ position of the microhomologous sequences (marked with upper lines in Table 2). During the end-joining process, after resection of strand ends, transient base-pairing at microhomologous sequences may occur and a few complementary bases at the 5′ position may also form base-pairing. In the absence of Parp-1, these base-pairings may be destabilized and resection and insertion of a few bases may tend to occur in the livers. Consistently of all seven simple-type deletions of two bases or more observed in the livers of *Parp-1*$^{-/-}$ mice (Table 1), none harbored a few complementary bases at the 5′ position of the microhomologous sequences (data not shown). On the other hand, in two simple-type deletions of two bases or more in *Parp-1*$^{+/+}$ mice, one deletion harbored a few complementary bases at the 5′ position of the microhomologous deletion junctions (Table 1).

In the brain, one out of three complex-type deletions of *Parp-1*$^{-/-}$ mice harbored microhomologous deletion junctions but did not harbor complementary bases at 5′ positions of the microhomologous deletion junctions. This point should be further evaluated by analyzing deletion mutations induced after treatment with various types of DNA damaging agents in different tissues.

The xeroderma pigmentosum complementation group A (Xpa) plays an important role in nucleotide excision repair (NER) and *Xpa*-deficient mice also show higher spontaneous mutant frequencies in the liver at advanced ages [40]. In fact, *Xpa*-deficient mice show an increased frequency of hepatocellular adenomas at older ages [34]. It is thus possible that endogenous DNA damage repairable by NER may occur during aging. However, no increase in the susceptibility to carcinogenesis induced in *Parp-1*$^{-/-}$ mice by 4-nitrosoquinoline1-oxide [41], which induces bulky DNA adducts, suggests that Parp-1 is not involved in NER.

Most liver cells stay in the G0 phase and they usually enter the cell division cycle after various stimulating events. An augmented frequency of DNA replication, like that in preneoplastic lesions, can also increase the chance of DSBs and may increase the frequency of deletions. Two of six *Parp-1*$^{-/-}$ mice used in the mutation analysis harbored tumors in the liver and the tumor regions were not included for DNA isolation. Because the frequencies and spectrum of mutations in the *gpt* or *red/gam* genes were unbiased in each mouse, we can exclude the possibility that the tissues used for isolation of DNA contained monoclonally proliferating preneoplastic lesions or other cycling cells.

It is also possible that an increased frequency of cell division may be causative of augmented frequency of DSBs and may result in a higher frequency of deletion mutation. However, if this is true, the observed mutation spectrum is expected to be the same between the genotypes. We could rule out this possibility because we observed different spectra of deletion mutations between the genotypes.

Unexpectedly we also found a 3-fold lower frequency of point mutations in adolescent *Parp-1*$^{-/-}$ compared to *Parp-1*$^{+/+}$ mice in the brain ($p = 0.009$). An age-dependent increase in the mutant frequency in *Parp-1*$^{-/-}$ mice was also shown ($p = 0.011$). Lower frequencies of G:C to A:T type mutation and deletion mutation in *Parp-1*$^{-/-}$ mice suggest that Parp-1 may be positively involved imprecise repair pathways which cause base substitution mutation of G:C to A:T and deletion mutation in the brain.

In conclusion, this result supports the view that Parp-1 is involved in suppressing imprecise repair of endogenous DNA damage leading to deletion mutation during aging in the liver and brain. *Parp-1*$^{-/-}$ mice show increased incidence of hepatocellular tumors at 18–24 months of ages [13]. The present results suggest a substantial role of Parp-1 in the maintenance of genomic stability and suppression of carcinogenesis during aging.

Conflict of interest

The authors declare that there are no conflicts of interest.

Acknowledgements

We are grateful to M. Abe for technical assistance, M. Yanagihara for maintenance of the animals and H. Suzuki and S. Gotoh for helpful suggestions on the manuscript. This work was supported in part by a Grant-in-Aid for the Cancer Research from the Ministry of Health, Labour and Welfare, a Grand-in-Aid from Third Term Comprehensive 10-Year Strategy for Cancer Control, and a Grant-in-Aid for Scientific Research from the Ministry of Education, Science, Sports, and Culture of Japan (16-11804).

References

[1] M. Masson, C. Niedergang, V. Schreiber, S. Muller, J. Menissier-de Murcia, G. de Murcia, XRCC1 is specifically associated with poly(ADP-ribose) polymerase and negatively regulates its activity following DNA damage, Mol. Cell. Biol. 18 (1998) 3563–3571.
[2] C. von Kobbe, J.A. Harrigan, V. Schreiber, P. Stiegler, J. Piotrowski, L. Dawut, V.A. Bohr, Poly(ADP-ribose) polymerase 1 regulates both the exonuclease and helicase activities of the Werner syndrome protein, Nucleic Acids Res. 32 (2004) 4003–4014.
[3] C. von Kobbe, J.A. Harrigan, A. May, P.L. Opresko, L. Dawut, W.H. Cheng, V.A. Bohr, Central role for the Werner syndrome protein/poly(ADP-ribose) polymerase 1 complex in the poly(ADP-ribosyl)ation pathway after DNA damage, Mol. Cell. Biol. 23 (2003) 8601–8613.
[4] S. Galande, T. Kohwi-Shigematsu, Poly(ADP-ribose) polymerase and Ku autoantigen form a complex and synergistically bind to matrix attachment sequences, J. Biol. Chem. 274 (1999) 20521–20528.
[5] B. Li, S. Navarro, N. Kasahara, L. Comai, Identification and biochemical characterization of a Werner's syndrome protein complex with Ku70/80 and poly(ADP-ribose) polymerase-1, J. Biol. Chem. 279 (2004) 13659–13667.
[6] L. Lan, S. Nakajima, Y. Oohata, M. Takao, S. Okano, M. Masutani, S.H. Wilson, A. Yasui, In situ analysis of repair processes for oxidative DNA damage in mammalian cells, Proc. Natl. Acad. Sci. U.S.A. 101 (2004) 13738–13743.
[7] S. Okano, L. Lan, K.W. Caldecott, T. Mori, A. Yasui, Spatial and temporal cellular responses to single-strand breaks in human cells, Mol. Cell. Biol. 23 (2003) 3974–3981.
[8] F. Le Page, V. Schreiber, C. Dherin, G. De Murcia, S. Boiteux, Poly(ADP-ribose) polymerase-1 (PARP-1) is required in murine cell lines for base excision repair of oxidative DNA damage in the absence of DNA polymerase beta, J. Biol. Chem. 278 (2003) 18471–18477.
[9] J.B. Leppard, Z. Dong, Z.B. Mackey, A.E. Tomkinson, Physical and functional interaction between DNA ligase IIIalpha and poly(ADP-Ribose) polymerase 1 in DNA single-strand break repair, Mol. Cell. Biol. 23 (2003) 5919–5927.
[10] M. Tsutsumi, M. Masutani, T. Nozaki, O. Kusuoka, T. Tsujiuchi, H. Nakagama, H. Suzuki, Y. Konishi, T. Sugimura, Increased susceptibility of poly(ADP-ribose) polymerase-1 knockout mice to nitrosamine carcinogenicity, Carcinogenesis 22 (2001) 1–3.
[11] T. Nozaki, H. Fujihara, M. Watanabe, M. Tsutsumi, K. Nakamoto, O. Kusuoka, N. Kamada, H. Suzuki, H. Nakagama, T. Sugimura, M. Masutani, *Parp-1* deficiency implicated in colon and liver tumorigenesis induced by azoxymethane, Cancer Sci. 94 (2003) 497–500.
[12] A. Gunji, A. Uemura, M. Tsutsumi, T. Nozaki, O. Kusuoka, K. Omura, H. Suzuki, H. Nakagama, T. Sugimura, M. Masutani, *Parp-1* deficiency does not increase the frequency of tumors in the oral cavity and esophagus of ICR/129Sv mice by 4-nitroquinoline 1-oxide, a carcinogen producing bulky adducts, Cancer Lett. 241 (2005) 87–92.
[13] W.M. Tong, U. Cortes, M.P. Hande, H. Ohgaki, L.R. Cavalli, P.M. Lansdorp, B.R. Haddad, Z.Q. Wang, Synergistic role of Ku80 and poly(ADP-ribose) polymerase in suppressing chromosomal aberrations and liver cancer formation, Cancer Res. 62 (2002) 6990–6996.
[14] W.M. Tong, U. Cortes, Z.Q. Wang, Poly(ADP-ribose) polymerase: a guardian angel protecting the genome and suppressing tumorigenesis, Biochim. Biophys. Acta 1552 (2001) 27–37.
[15] W.M. Tong, H. Ohgaki, H. Huang, C. Granier, P. Kleihues, Z.Q. Wang, Null mutation of DNA strand break-binding molecule poly(ADP-ribose) polymerase causes medulloblastomas in p53(−/−) mice, Am. J. Pathol. 162 (2003) 343–352.
[16] M.E. Dolle, W.K. Snyder, J.A. Gossen, P.H. Lohman, J. Vijg, Distinct spectra of somatic mutations accumulated with age in mouse heart and small intestine, Proc. Natl. Acad. Sci. U.S.A. 97 (2000) 8403–8408.
[17] K.A. Hill, V.L. Buettner, A. Halangoda, M. Kunishige, S.R. Moore, J. Longmate, W.A. Scaringe, S.S. Sommer, Spontaneous mutation in Big Blue mice from fetus to old age: tissue-specific time courses of mutation frequency but similar mutation types, Environ. Mol. Mutagen. 43 (2004) 110–120.
[18] T. Ono, H. Ikehata, S. Nakamura, Y. Saito, Y. Hosoi, Y. Takai, S. Yamada, J. Onodera, K. Yamamoto, Age-associated increase of spontaneous mutant frequency and

Please cite this article in press as: A. Shibata, et al., Role of Parp-1 in suppressing spontaneous deletion mutation in the liver and brain of mice at adolescence and advanced age, Mutat. Res.: Fundam. Mol. Mech. Mutagen. (2009), doi: 10.1016/j.mrfmmm.2009.02.001